Y 3. N21/5 : 6/3341

GOVT. DOC.

BUSINESS AND
TECHNICAL DEPT.
Dec 6 '54

NATIONAL ADVISORY COMMITTEE FOR AERONAUTICS

TECHNICAL NOTE 3341

AN ANALYTICAL ESTIMATION OF THE EFFECT OF TRANSPIRATION COOLING ON THE HEAT-TRANSFER AND SKIN-FRICTION CHARACTERISTICS OF A COMPRESSIBLE, TURBULENT BOUNDARY LAYER

By Morris W. Rubesin

Ames Aeronautical Laboratory
Moffett Field, Calif.

NACA

Washington

December 1954

NATIONAL ADVISORY COMMITTEE FOR AERONAUTICS

TECHNICAL NOTE 3341

AN ANALYTICAL ESTIMATION OF THE EFFECT OF TRANSPIRATION COOLING ON THE HEAT-TRANSFER AND SKIN-FRICTION CHARACTERISTICS OF A COMPRESSIBLE, TURBULENT BOUNDARY LAYER

By Morris W. Rubesin

SUMMARY

An analysis based on mixing-length theory is presented which indicates that surface blowing associated with transpiration cooling systems produces large reductions in both the heat-transfer and skin-friction coefficients for a turbulent boundary layer on a flat plate. The numerical results are restricted to the case of air blowing into air. The effects of blowing are indicated to be similar for high-speed, compressible flow to those for low-speed, incompressible flow.

INTRODUCTION

The frictional heating of the outer surfaces of high-speed aircraft has become a major problem in the design of these aircraft. Without thermal protection and at equilibrium conditions, the surfaces of these aircraft will begin reaching intolerable temperatures at Mach numbers even as low as 2. The designer, therefore, must provide thermal protection for his aircraft's skin. This protection can be achieved in several ways; for example, by altering the aircraft's shape to avoid sharp or pointed frontal surfaces, by providing a cooling system for the skin, and by providing a protective thermal insulating layer between the hot air in the boundary layer and the skin. A transpiration cooling system, one in which the coolant passes through small pores in the skin and into the outside boundary layer, has the advantage of providing both cooling of the skin and a protective insulating layer of coolant. It appears that these advantages make a transpiration cooling system most effective (ref. 1). It is noted that the advantage of evaporation can also be incorporated into a transpiration cooling system.

Much of the available work dealing with transpiration cooling is restricted to analyses dealing with the laminar boundary layer. The literature is quite extensive and references 2 and 3 represent examples of these analyses. Investigations which are more allied to the work

presented in this paper are represented by references 4, 5, and 6.[1] These analyses treat the case of the turbulent boundary layer by dividing the boundary layer into two parts, a laminar sublayer and a fully turbulent outer region. The end results of these analyses, in effect, relate the coefficient of heat transfer under conditions of transpiration with two parameters; namely, (1) the velocity at the interface of the sublayer and outer turbulent portion and (2) a Reynolds number based on the distance of this interface from the surface with properties evaluated either at the wall or free-stream temperature. The rate of transpiration acts as an independent variable in the latter relation. Because it is known that both of these parameters are dependent on the local skin friction for the case of zero transpiration, it would be expected that their partial dependence on the local skin friction would continue even under the conditions of transpiration. In effect, then, the results of these analyses are modified Reynolds analogies relating heat transfer and skin friction when blowing occurs. A similar analysis comprises a portion of this report; however, it is modified to also include the frictional dissipation occurring in the high-speed air flow over the surfaces of aircraft.

Several experiments have been performed concerning transpiration cooling in tubes or channels having turbulent boundary layers (refs. 5, 7, and 8). Although the results point out the advantages of transpiration cooling, the geometry of the tests and the low velocities employed in the boundary layer make the results of these tests too specific to apply in the general case of aircraft. The experiment described in reference 9, although also employing low air speeds, provides data on a flat plate, which is a fundamental aerodynamic shape. These data will be compared with the present analysis in a later portion of this report.

From this brief review of literature dealing with transpiration cooling, it is apparent that there is no information about the influence of transpiration on the behavior of a compressible, turbulent boundary layer, such as exists on the surface of a high-speed aircraft. The purpose of the present report is to present an approximate analysis for determining the effect of transpiration on a high-speed turbulent boundary layer. Because of the many uncertainties inherent in the analysis, it mainly has heuristic value. Experimental data will be required before the value of the analysis as a means of interpolating or extrapolating limited amounts of data can be assessed.

---

[1]A simultaneous investigation, essentially the same as is contained in portions of the present report, has been reported recently in an article by W. H. Dorrance and F. J. Dore, entitled "The Effect of Mass Transfer on the Compressible Turbulent Boundary Layer Skin Friction and Heat Transfer." Jour. Aero. Sci., vol. 21, no. 6, June 1954.

SYMBOLS

a	arbitrary constant
A	parameter, $\sqrt{\frac{\frac{\gamma-1}{2}M_1^2}{T_W/T_1}}$
b	arbitrary constant
B	parameter, $\frac{1+\frac{\gamma-1}{2}M_1^2}{T_W/T_1}-1$
c_p	specific heat at constant pressure
c_f	local skin-friction coefficient
f	ratio, $\frac{St}{c_f/2}$, defined by equation (10)
F	elliptic integral of the first kind
g	exponential term defined by equation (A33) and (A34) in Appendix A
G	function defined by equation (6)
h	local heat-transfer coefficient defined by equation (A78)
k	thermal conductivity
k_m, k_n	parameters of elliptic integral of first kind (see eqs. (A66) and (A68))
K	mixing length parameter, $l = Ky$
l	mixing length
M	Mach number
Pr	Prandtl number, $\frac{\mu c_p}{k}$
Pr_t	turbulent Prandtl number, $\frac{\epsilon_M c_p}{\epsilon_H}$

q local heat-transfer rate per unit area

r local temperature recovery factor (see eq. (A80))

R_x Reynolds number based on distance along plate and free-stream fluid properties

R_θ Reynolds number based on momentum thickness and free-stream fluid properties

St local Stanton number, $\frac{h}{\rho_1 u_1 c_p}$

T temperature

u velocity component parallel to plate

v velocity component perpendicular to surface of plate

x coordinate parallel to axis of plate

y coordinate perpendicular to surface of plate

α parameter defined by equation (A58)

β parameter defined by equation (A59)

γ ratio of specific heats, 1.40 for air

ϵ_H eddy thermal conductivity, defined by equation (A11)

ϵ_M eddy viscosity, defined by equation (A10)

ζ constant relating transpiration rate with local skin-friction coefficient, $\frac{\rho_w v_w / \rho_1 u_1}{c_f/2}$

θ momentum thickness

μ viscosity

ρ mass density

σ parameter defined by equation (A60), ζ^{-1}

τ local shear stress

φ_m, φ_n parameter of elliptic integral of first kind

ω exponent in viscosity - temperature relationship

Superscripts

' instantaneous fluctuating quantity

- quantity averaged with respect to time

+ dimensionless quantity (see eqs. (A26) and (A27))

~ dimensionless quantity (see eq. (A19))

Subscripts

a interface of laminar sublayer and outer turbulent region

c coolant fluid initial condition

e temperature recovery condition, $T_e = T_1 + r \frac{u_1^2}{2c_p}$

W surface

1 outer edge of boundary layer

ANALYSIS

Restrictions on Analysis

The present analysis has several restrictions which have been imposed because of inherent difficulties or for purposes of simplification. These restrictions are as follows:

1. Only the compressible, turbulent boundary layer is considered (usual boundary-layer assumptions).

2. The boundary layer is on a flat plate placed parallel to the free-stream direction.

3. The coolant fluid is the same as the boundary-layer fluid and enters the boundary layer at the temperature of the surface of the plate (no diffusion).

4. The boundary layer is idealized to be composed of two distinct sections: a laminar sublayer next to the surface, and a fully turbulent outer layer. (Note: It is assumed that velocity, temperature, heat flux, and shear are continuous at the interface of the two layers.)

5. In the fully turbulent outer layer, the transport of heat is proportional to the transport of momentum.

Parts of the Analysis

For relative simplicity the analysis is divided into two parts. The first part contains a determination through the use of mixing-length theory of the effect of transpiration on skin friction and heat transfer in a compressible turbulent boundary layer when the Prandtl number is unity. The assumption Pr = 1 greatly simplifies this portion of the analysis. The second part contains a determination of the effect of transpiration on the relation between the coefficients of skin friction and heat transfer when the Prandtl number is not unity. An expression for temperature recovery factor is also found in the second part.

A combination of the results of the two parts (the product of c_f when Pr = 1 and St/c_f when Pr $\neq$ 1) allows the determination of the local heat-transfer coefficients under the conditions of transpiration when Prandtl number is not unity. To permit this combination, it is necessary to employ the premise that the local skin-friction coefficient is relatively independent of Prandtl number. For the case with no transpiration, this premise is good for a Prandtl number which corresponds to air (ref. 10). It is not expected that small amounts of transpiration should alter the basic premise.

Description of Method of Analysis

This description of the analysis is intended to point out its salient features without introducing the complexities of the detailed mathematics. The mathematical details may be found in Appendix A.

The basic equations that are used in this analysis are the Navier-Stokes equations representing conservation of momentum, the conservation of energy equation, and the continuity or conservation of mass equation. When all the quantities in these equations are represented as the sum of a time averaged quantity plus an instantaneous quantity, these equations can be made to apply to turbulent flow (ref. 11). When these "turbulent flow" equations are time averaged and the usual boundary-layer assumptions are imposed, the resulting boundary-layer equations are (ref. 10):

$$\frac{\partial}{\partial x}(\bar{\rho}\bar{u}) + \frac{\partial}{\partial y}(\bar{\rho}\bar{v} + \overline{\rho' v'}) = 0 \tag{1}$$

$$\bar{\rho}\bar{u}\frac{\partial \bar{u}}{\partial x} + (\bar{\rho}\bar{v} + \overline{\rho' v'})\frac{\partial \bar{u}}{\partial y} = \frac{\partial}{\partial y}\left(\bar{\mu}\frac{\partial \bar{u}}{\partial y} - \bar{\rho}\overline{u' v'}\right) \tag{2}$$

$$\bar{\rho}\bar{u}\frac{\partial}{\partial x}\left(c_p\bar{T} + \frac{\bar{u}^2}{2}\right) + (\bar{\rho}\bar{v} + \overline{\rho' v'})\frac{\partial}{\partial y}\left(c_p\bar{T} + \frac{\overline{u^2}}{2}\right) = \frac{\partial}{\partial y}\left(\bar{k}\frac{\partial \bar{T}}{\partial y} + \bar{\mu}\bar{u}\frac{\partial \bar{u}}{\partial y} - \bar{\rho}c_p\overline{v' T'} - \bar{u}\bar{\rho}\overline{u' v'}\right) \tag{3}$$

Barred quantities represent time averages, while primed quantities represent instantaneous values of fluctuating quantities. While the specific heat is maintained constant, the fluid properties of density, viscosity, and thermal conductivity are allowed to vary with temperature. Frictional dissipation is also included.

Equations (1) through (3) are intractable at present, because of their complexity and because the behavior of the turbulent fluctuating components in shear flow is not known. Certain nonrigorous simplifications are necessary to achieve a solution useful from an engineering viewpoint.

The first simplification necessary in achieving an engineering solution to the problem is to assume in equations (1) through (3) that the variations of the dependent variables with respect to x are negligible compared to their variations with respect to y in the evaluation of the local velocity distribution. This allows replacing partial differential equations by much more easily solved ordinary differential equations, with y as the independent variable. The above assumption is based on experience with the low-speed, incompressible skin-friction problem without transpiration. It has been found that this assumption combined with a group of assumptions concerning the mechanism of turbulence and the structure of the boundary layer together with certain mathematical simplifications can be made to yield skin-friction coefficients which agree well with the experimental results.

At this point it is necessary to define the Prandtl number as it is used in this report. In the conventional definition Prandtl number is the ratio of kinematic viscosity to the thermal diffusivity of a fluid where the transport of momentum and heat is promoted by molecular means. This Prandtl number is then a controlling variable for processes containing laminar flow where molecular transport phenomena occur. When the flow is turbulent, however, the large-scale transport of momentum and heat is promoted by the eddying motion, and the conventional Prandtl number does not govern this mechanism. In order to relate the turbulent

transport of momentum and heat transfer, it is necessary to define a new term which has the same characteristics as Prandtl number, except that properties defining the term are based on eddying motion. To distinguish this term from the conventional Prandtl number, it is called the turbulent Prandtl number. A turbulent Prandtl number of unity is equivalent to the Reynolds analogy.

When the basic equations are reduced to ordinary differential equations, they are applied to the fully turbulent outer layer by omitting all the terms which are based on molecular transport. In the laminar sublayer, however, all the terms based on eddying transport are omitted. Thus, two sets of equations are employed, the solutions of each being matched at the interface of the two layers. Experience has shown that this two-layer model of a turbulent boundary layer is quite good as long as both the Prandtl number and turbulent Prandtl number are close to unity.

At this stage, the analysis is divided into two parts. In the first part it is assumed that Prandtl number and turbulent Prandtl number are both equal to unity, which results in a direct relationship between the temperature and velocity. Because of this relationship, it is not necessary to solve the energy equation. The momentum equation is solved together with the continuity equation to yield the velocity (and temperature) distribution through the boundary layer with the local surface shear as a parameter. The velocity distribution is then substituted in the integral expression for the momentum thickness. As this integral is not readily solvable in closed form, the first term of a series solution is employed. The first term represents an asymptotic solution for the case of extremely low values of the skin-friction coefficient and low rates of transpiration; that is, $\sqrt{c_f/2} << 1$ and $\sqrt{(\rho_w v_w/\rho_1 u_1)} << 1$. Thus, a relationship is obtained between the local skin-friction coefficient and Reynolds number with the momentum thickness as the characteristic dimension. When the von Kármán momentum-integral equation is integrated using the relationship $c_f(R_\theta)$, there results an expression for the local skin-friction coefficient in terms of a Reynolds number using the length along the plate as the characteristic dimension. This latter integration is also not made in closed form, the first term of a series expansion again being used as an asymptotic relationship for small values of the skin-friction coefficient and the transpiration rate. The first part of the analysis, consequently, results in the determination of the effect of transpiration on the relationship $c_f(R_x)$ when Pr and Pr_t are both unity.

It is known that the local heat-transfer coefficient is dependent on Pr and Pr_t. To evaluate this dependence, the second part of the analysis is performed to determine the relationship between the local Stanton number and the local skin-friction coefficient under conditions of transpiration when Pr and Pr_t are not unity. This is achieved by

taking the ratio of members of the energy equation to corresponding members of the momentum equation. The ratio of the members forms an ordinary differential equation relating total energy and velocity. When the differential equation is integrated in closed form across the boundary layer, there is obtained a relationship between Stanton number and the local skin-friction coefficient. An ancillary result is an expression for the local temperature recovery factor.

A combination of the two parts of the analysis provides $St(R_x)$ under conditions of transpiration for Prandtl numbers other than unity.

Summary of Results of Analysis

The results of part I of the analysis can be summarized as follows:

$$\ln \frac{R_\theta K}{y_a^+ \sqrt{1 + \frac{\rho_w v_w / \rho_1 u_1}{c_f/2}}} = G \tag{4}$$

or

$$\ln \frac{K \sqrt{\frac{c_f}{2}\left(\frac{c_f}{2} + \frac{\rho_w v_w}{\rho_1 u_1}\right) R_x}}{y_a^+} = G \tag{5}$$

where

$$G = \frac{2K\left(\frac{T_1}{T_W}\right)^{1/2}}{A\sqrt{\frac{\rho_W v_W}{\rho_1 u_1}}\sqrt{\beta - \alpha}}\left\{F[k_m, \varphi_m(\tilde{u}_a)] - F[k_m, \varphi(1)]\right\}$$

when

$$k_m^2 = \frac{\beta + \sigma}{\beta - \alpha} < 1$$

$$\sin^2\varphi_m = \frac{\beta - \tilde{u}}{\beta + \sigma}$$

or

$$G = \frac{2K\left(\frac{T_1}{T_W}\right)^{1/2}}{A\sqrt{\frac{\rho_W v_W}{\rho_1 u_1}}\sqrt{\beta + \sigma}}\left\{F[k_n, \varphi_n(\tilde{u}_a)] - F[k_n, \varphi_n(1)]\right\}$$

when

$$k_n^2 < \frac{\beta - \alpha}{\beta + \sigma} < 1$$

$$\sin^2\varphi_n = \frac{\beta - \tilde{u}}{\beta - \alpha}$$

(6)

Note:

$$\alpha = \frac{B - \sqrt{B^2 + 4A^2}}{2A^2}$$

$$\beta = \frac{B + \sqrt{B^2 + 4A^2}}{2A^2}$$

$$\sigma = \frac{(c_f/2)}{\left(\frac{\rho_W v_W}{\rho_1 u_1}\right)}$$

The term $F(k,\varphi)$ is an elliptic integral of the first kind.

For the values of K, y_a^+, and $\tilde{u}_a$ to be used in the above see "DISCUSSION" (note $\tilde{u}_a = u_a^+\sqrt{c_f/2}$). The results of part II of the analysis can be summarized as follows:

$$\frac{St}{\left(\frac{c_f}{2}\right)} = \frac{\left(\frac{\rho_W v_W}{\rho_1 u_1}\right)}{\left(\frac{c_f}{2}\right)^{1-Pr}\left(\frac{\rho_W v_W}{\rho_1 u_1}\tilde{u}_a + \frac{c_f}{2}\right)^{Pr-Pr_t} - \frac{c_f}{2}} \tag{7}$$

$$r = 1 - 2\,\frac{\left(\frac{\rho_W v_W}{\rho_1 u_1}\right)\left(\frac{\rho_W v_W}{\rho_1 u_1}+\frac{c_f}{2}\right)(2-Pr)(2-Pr_t) - (2-Pr)\left(\frac{\rho_W v_W}{\rho_1 u_1}+\frac{c_f}{2}\right)^2 + \left(\frac{\rho_W v_W}{\rho_1 u_1}\tilde{u}_a+\frac{c_f}{2}\right)^{2-Pr_t}\left(\frac{\rho_W v_W}{\rho_1 u_1}+\frac{c_f}{2}\right)^{Pr_t}(Pr_t-Pr)}{\left(\frac{\rho_W v_W}{\rho_1 u_1}\right)^2(2-Pr_t)(2-Pr)} -$$

$$2\,\frac{(2-Pr_t)\left(\frac{c_f}{2}\right)^{2-Pr}\left(\frac{\rho_W v_W}{\rho_1 u_1}\tilde{u}_a+\frac{c_f}{2}\right)^{Pr-Pr_t}\left(\frac{\rho_W v_W}{\rho_1 u_1}+\frac{c_f}{2}\right)^{Pr_t}}{\left(\frac{\rho_W v_W}{\rho_1 u_1}\right)^2(2-Pr_t)(2-Pr)} \tag{8}$$

DISCUSSION

Evaluation of K, u_a^+, y_a^+

The end results of the analysis, as represented by equations (4) through (8), are entirely general until specific values of K, u_a^+, and y_a^+ are selected. This means that before numerical answers can be determined from this analysis, information other than that contained in the analysis must be employed. This information, that is, the values of K, u_a^+, and y_a^+, must be determined from experiment. Thus, the numerical results of this report can at best be as good as the experiments used in selecting K, u_a^+, and y_a^+.

Low-speed case with no transpiration.- For the incompressible, zero transpiration case K, u_a^+, and y_a^+ can be evaluated in three ways. The first way is from velocity-distribution data, where K is a measure of the rate of increase of the velocity with distance from the surface, and u_a^+ and y_a^+ are the conditions at the interface of the sublayer and outer turbulent portion. The second way is from $c_f(R_\theta)$ data. In this evaluation the terms K, u_a^+, and y_a^+ lose some of their physical significance in that they may be considered as arbitrary constants which absorb some of the inaccuracies introduced by the mathematical simplifications employed in evaluating the momentum thickness from the velocity-distribution data. The third way is from $c_f(R_x)$ data where, again, K, u_a^+, and y_a^+ are treated as arbitrary constants, absorbing still other mathematical simplifications.

The experimental velocity-distribution data can be plotted in the dimensionless form u^+ vs. y^+ when local surface shear stresses have been obtained simultaneously. By choosing K, u_a^+, and y_a^+ appropriately, the analysis can be made to fit portions of the boundary-layer data very well. If the quantities K, u_a^+, and y_a^+ are adjusted so that the inner portion of the turbulent layer is well represented, the analysis, however, will not fit the data in the outer portion of the layer, and vice versa. This lack of agreement between analysis and experiment is not entirely surprising when it is recalled that the analysis is based on a primitive mixing-length theory and that several mathematical simplifications have been imposed.

Before the experimental data of $c_f(R_\theta)$ or $c_f(R_x)$ can be used to evaluate the arbitrary quantities, it is necessary to relate u_a^+ and y_a^+ analytically. This is necessary because the skin-friction data will only supply either K and u_a^+ or K and y_a^+ with sufficient accuracy. For the incompressible, no transpiration case, a comparison of the quantities evaluated in the three different manners is shown in the following table:

	From velocity survey data (inner portion of turbulent layer)	From $c_f(R_\theta)$ data	From $c_f(R_x)$ data
K	0.400	0.352	0.392
$u_a^+ = y_a^+$	11.5	12.6	13.1

These values were evaluated from figures of data summarized in reference 12. It is apparent that the values of K and u_a^+ given by the alternative methods do not agree, the extreme values of K differing by about 14 percent and the extreme values of u_a^+ also differing by about 14 percent. These differences, undoubtedly, are due to the inadequacies of the mixing-length theory and the mathematical approximations imposed.

For the purposes of the present report, however, the chief concern is adequate representation by the analysis of $c_f(R_x)$. In figure 1, there has been reproduced a figure from reference 12 showing available data of $c_f(R_x)$. The curves given by the present analysis are represented by solid lines. The analytical line based on $c_f(R_\theta)$ data differs from the $c_f(R_x)$ data by less than 7 percent. The analytical line, based on velocity-distribution data, is about 12-percent higher than the $c_f(R_x)$ data. From this it can be inferred that no matter which method is employed to obtain K, u_a^+, and y_a^+, use of these values to obtain $c_f(R_x)$ will result in answers adequate for engineering purposes.

Low-speed case with transpiration.- There exist insufficient data to define precisely the effect of transpiration on K, u_a^+, and y_a^+. The data of reference 9 do not allow these determinations even though they include temperature-distribution surveys, velocity-distribution surveys, and measurements of local heat transfer. The temperature-distribution data were not used because evaluating K, u_a^+, and y_a^+ from temperature-distribution surveys and local surface heat-transfer measurements requires making assumptions concerning the analogy between heat transfer and momentum transfer. Examination of the velocity-distribution data revealed that local skin-friction coefficients were more than 20 percent higher than the values in figure 2 for the case with zero transpiration. These high values were attributed to surface roughness effects. Since it is not known how roughness is affected by transpiration, it is believed that the velocity-distribution data may include the effects of both. Because heat transfer in turbulent flow seems to be affected by roughness to a much lesser extent than is skin friction (ref. 13), it was decided to employ the heat-transfer data in the evaluation of K, u_a^+, and y_a^+. As the data are not sufficiently precise to do this directly, it was necessary to employ the alternative approach of postulating values of K, u_a^+, and y_a^+ and then of comparing the end results with the data of reference 9. Physical considerations were employed in guiding these postulates.

From the physical viewpoint it would be expected that u_a^+ and y_a^+ should be consistent with the velocity-distribution curve within the sublayer, equation (A25). In addition it would be expected that the Reynolds number at the outer edge of the sublayer, based on the thickness of the sublayer and equal to $u_a^+ y_a^+$, should be nonincreasing under the disturbing influence of transpiration. Consequently, the two assumptions investigated are:

(a) $u_a^+ y_a^+ = (13.1)^2$ solved simultaneously with equation (A25) and

(b) $u_a^+ = 13.1$ and y_a^+ from equation (A25).

The first of these represents the case of a constant sublayer Reynolds number, while the second corresponds to a Reynolds number which becomes smaller as the transpiration rate is increased. A comparison of the individual results based on these assumptions provides an indication of the influence the assumptions concerning the sublayer may have. To examine this point further, other numerical results were obtained using the condition that $u_a^+ = y_a^+ = 13.1$, identical with the no transpiration case. It should be noted that this latter condition is inconsistent with the sublayer equation (eq. (A25)).

Besides the question of the boundary conditions at the outer edge of the sublayer, there exists the problem of choosing a value of K, the mixing-length parameter, under the conditions of transpiration. Only well-defined experiments can answer this problem and, at present, the only recourse available is to assume it is unchanged by the transpiration; namely, $K = 0.392$. In addition to these assumptions, the conditions $M = 0$, $T_W/T_1 = 1$, $Pr = 0.72$, and $Pr_t = 1.00$ are imposed on the analysis to make it conform with the test conditions of reference 9.

Comparison with Data

A comparison of the data and analysis is shown in figure 2 for the case where the transpiration rate, $\rho_W v_W/\rho_1 u_1$, is equal to zero. The local Stanton number is plotted as a function of Reynolds number with the distance along the channel wall used as the characteristic dimension. It appears that the data of run H-1 correspond to a laminar boundary layer; the data of runs H-2 and H-3 correspond to a boundary layer which is laminar at the lower Reynolds numbers and transforms to one that is turbulent at the higher Reynolds numbers; and the data of run H-4 correspond to a boundary layer which has become turbulent very close to the leading edge of the channel wall. When the data of run H-1 are compared with Pohlhausen's theoretical result for laminar flow, it is noted that the data are generally about 20-percent higher than theory. Since Pohlhausen's theory was checked experimentally in the past by Fage and Falkner (ref. 14), some doubt is raised concerning the accuracy of the data with laminar flow. The data corresponding to turbulent flow,

however, agree fairly well with the well-known empirical Colburn curve, reference 15, or with a curve derived from the present analysis (note for case where $\rho_W v_W/\rho_1 u_1 = 0$, various postulates about the sublayer are identical). The deviations shown by the high Reynolds number data for each of runs H-3 and H-4 are not considered.

For the purpose of the present paper, the main point is consideration of the agreement of the data corresponding to turbulent flow with the results of the present analysis. It should be emphasized that for comparison purposes the data should actually be plotted against a Reynolds number in which the characteristic dimension is the effective length of a fully turbulent boundary layer. The effective length is defined as the distance along the flat plate where a boundary layer, fully turbulent from the start, would have the same Stanton number as the actual boundary layer for which transition from laminar to turbulent flow has occurred downstream of the leading edge. The data given in reference 9 are insufficient to define precisely the effective start of turbulence, so it is necessary to resort to estimates. Because the Stanton number approaches infinity as Reynolds number approaches zero, any of the data points corresponding to turbulent flow having a finite value of Stanton number are downstream of the effective starting point of the turbulent boundary layer. Thus, if the effective starting point of a fully turbulent boundary layer is chosen as the point where the data indicate transition has just ended and the flow is completely turbulent, the effective-length Reynolds number so determined would certainly be smaller than the true effective Reynolds number. When this extreme correction is applied to the data, that is, 1.8×10^5 is subtracted from the R_x for run H-2, 9×10^4 is subtracted from the R_x for run H-3, and the R_x of run H-4 are left unchanged, it is found that the data cluster near the analytical result with a spread of about 20 percent as shown in figure 3. The results based on the correct effective starting length would undoubtedly lie between those shown in figures 2 and 3 and would be in good agreement with the proposed analytical method, considering the inherent scatter in the data.

Before a comparison of the proposed analytical method and the data can be made under conditions of transpiration, it is necessary to discuss aspects of the variation of the transpiration rate along the surface of a plate. If it is assumed that both conduction within the porous surface and radiation are negligible, a heat balance on a portion of the porous surface results in the following equation:

$$St(T_e - T_W) = \frac{\rho_W v_W}{\rho_1 u_1}(T_W - T_c) \tag{9}$$

Because St varies with x, it is apparent that if T_e and T_c are constant with respect to distance along the plate, the only condition compatible with a constant surface temperature is $\rho_W v_W/\rho_1 u_1 = \epsilon St$

where ϵ is a constant of proportionality. On the contrary, if $\rho_W v_W/\rho_1 u_1$ = constant, the surface temperature T_W will vary along the surface of the plate.

In the present analysis it is quite inconvenient to treat the first of these cases exactly. This arises from the fact that the analysis is divided into two parts, that is, the local Stanton number is determined from a local skin-friction coefficient that was determined for the particular case of $Pr = Pr_t = 1$ and a prescribed variation of $\rho_W v_W/\rho_1 u_1$. Thus, to make $\rho_W v_W/\rho_1 u_1 = \epsilon St$ would require an iteration process. For convenience, and because it does not produce a large error in the practical case, the relationship

$$\frac{St}{\left(\frac{c_f}{2}\right)} = f \equiv f\left(Pr,\ Pr_t,\ \frac{\rho_W v_W}{\rho_1 u_1},\ M\right) \tag{10}$$

will be assumed. This assumption implies that the Reynolds number dependence of the function f is negligible. It will be shown later that although this is not exactly true, the assumption only introduces an error of about ± 4 percent over the Reynolds number range of the experiments in reference 9. When equation (10) is introduced into equation (9) there results:

$$T_e - T_W = \frac{\left(\frac{\rho_W v_W}{\rho_1 u_1}\right)}{\left(\frac{c_f}{2}\right) f} (T_W - T_c) \tag{11}$$

Thus letting $\rho_W v_W/\rho_1 u_1 = \zeta(c_f/2)$ results in essentially a constant surface temperature, where ζ is a constant of proportionality.

For the case where the fluid properties are essentially constant, that is, low-speed flow with small temperature variations, it is possible to apply the analysis directly to the case where $\rho_W v_W/\rho_1 u_1$ = constant. Some error will occur because of neglecting the effect of axial variations in the surface temperature on the convective heat transfer. For the case with zero transpiration, it is known that continuous variations of surface temperature have little effect on heat transfer in a turbulent boundary layer (ref. 16). It is not expected that small amounts of transpiration should markedly alter this. Thus, the results provided by the analysis for $\rho_W v_W/\rho_1 u_1$ = constant should be applicable for comparison with the data of reference 9.

Comparisons of the analytical results with the data of reference 9 are presented in figures 4, 5, 6, and 7. Figures 4 and 5 correspond to constant $\rho_w v_w/\rho_1 u_1$, and figures 6 and 7 correspond to $\rho_w v_w/\rho_1 u_1 = \zeta(c_f/2)$. In these figures no corrections for the effective starting length have been made for the Reynolds numbers of the data.

In figure 4 the variation of Stanton number with length Reynolds number is shown for $\rho_w v_w/\rho_1 u_1 = 0.002$. The analytical results based on the assumed conditions of K, u_a^+, and y_a^+ are also included. It is surprising how well either postulate compatible with the sublayer equation compares with the data. The analysis with either of these postulates gives about the correct order of magnitude for the reduction in Stanton number due to transpiration and, in addition, indicates the larger variation in Stanton number with changes in Reynolds number. The differences in the analytical results and the data are shown much more clearly in figure 5 where $\rho_w v_w/\rho_1 u_1 = 0.006$. In this figure neither analytical result based on either postulate agrees well with the data, however, both analytical results indicate a large reduction in St and a larger variation of St with R_x, as is exhibited by the data. It is interesting that the two analytical results bracket the data. In both figures, however, the postulate where the sublayer is considered unchanged by transpiration leads to analytical results which exhibit the poorest agreement with the data. Another point of interest is a confirmation that variations in surface temperatures affect the data to a small degree. This is seen from a comparison in figure 4 of runs 17b and 20b with runs 16a, 17a, and 20a, where the differences between a constant surface temperature and a variable surface temperature are masked by the scatter of the data. The results of figure 5 further substantiate this point.

In figures 6 and 7 the variation of Stanton number with length Reynolds number is shown for $\rho_w v_w/\rho_1 u_1 = \zeta(c_f/2)$. In view of the previous results, only the analytical results based on postulates compatible with the sublayer are compared with the data. To agree with the experimental values of ζ the values of ζ for the two cases are 1.04 and 1.15, respectively, in figure 6. The corresponding values of ζ in figure 7 are $\zeta = 2.68$ and 3.34. Although the data scatter markedly, a comparison of the data and analysis is quite favorable when consideration is made of the probable effective starting point of the data of run H-10.

From the above comparison of data of reference 9 with the results of the present analysis, it can be concluded that for the low speed, incompressible case, answers sufficiently accurate for engineering purposes can be provided by the analysis when the arbitrary constants of the analysis are set equal to:

$$K = 0.392$$

$$u_a^+ = 13.1$$

and y_a^+ is determined from equation (A25). It will be noted that a postulate considering the sublayer Reynolds number variable is employed in preference to a postulate where it is considered constant. This is done from the viewpoint of providing a more conservative answer (i.e., less reduction in St with transpiration) than is exhibited by the bulk of the data.

Examples of Results of Analysis, Including Extensions to High-Speed, Compressible Flow

Examples of the effect of transpiration on the local skin-friction coefficient, the ratio of Stanton number to the skin-friction coefficient, and the local recovery factor are shown in figures 8, 9, and 10. These curves include cases of Mach number equal to 0, 2, and 4. The curves shown are subject to the following conditions:

(a) $K = 0.392$

(b) $u_a^+ = 13.1\sqrt{\frac{T_W}{T_1}}$

(c) y_a^+ is determined from equation (A25)

(d) $\omega = 0.8$

For figure 8 the conditions for Prandtl number are:

(e) $Pr = 1.00$

(f) $Pr_t = 1.00$

In figures 9 and 10 the conditions for Prandtl number are:

(g) $Pr = 0.72$

(h) $Pr_t = 1.00$

In all the figures, the parameter of the curves is the dimensionless transpiration parameter $\zeta = \frac{(\rho_W v_W/\rho_1 u_1)}{(c_f/2)}$. This condition of constant ζ, implying a varying transpiration rate along the surface, was chosen for the examples from the practical viewpoint that it requires a smaller amount of transpiration air to maintain a certain maximum surface

temperature over a region than does a constant transpiration rate system. Two surface-temperature conditions are presented: the first, is where the surface is at the total temperature and the second is where the surface temperature is at the free-stream static temperature. These surface temperatures are certainly the extreme limits of the range of temperatures likely to be encountered on the surface of a cooled aircraft.

Conditions (a) through (c) are essentially the same as postulate (b) (page 14) defined previously, except that u_a^+ is based on fluid properties evaluated at the surface temperature. This accounts for the temperature-ratio term in (b). Condition (d) represents the viscosity exponent corresponding approximately to conditions occurring in flight. Conditions (e) and (f) were chosen for purposes of mathematical simplification while (g) corresponds to air and (h) implies an exact Reynolds analogy in the outer turbulent layer.

It is apparent from figure 8 that transpiration has a very strong effect on lowering the value of the local skin-friction coefficient at all the Mach numbers considered and at both surface-temperature conditions. As an example, at $M = 4$ where $T_W = T_1$, the local skin-friction coefficient at $R_x = 10^7$ is reduced to around 15 percent of its original value by a blowing rate of $\rho_W v_W/\rho_1 u_1 \cong 0.003$ ($\zeta = 20$).

From figure 9 it is seen that the effect of transpiration at all the conditions considered is to increase the ratio of Stanton number to the local skin-friction coefficient when $Pr = 1$. This increase is of a much smaller magnitude than the decrease in the local skin-friction coefficient, with the net result being that the Stanton number is also markedly reduced by transpiration. For example, at the point previously considered, the Stanton number falls to about 21 percent of its original value.

In figure 10 there is shown a series of curves for the local recovery factor at $M = 0$. This figure is representative of all the other conditions considered, and the following discussion applies in general. From the figure it is noted that transpiration also affects the recovery factor; however, it can be observed that the effect of transpiration is not too large. In fact, the transpiration effect is much less than the apparent effect of Reynolds number for the zero transpiration case. Since it is known from experiment (ref. 10) that the recovery factor at zero transpiration is relatively independent of Reynolds number, doubt is shed on the validity of the recovery-factor determinations of this analysis. From a consideration of relative results, all that can be concluded is that transpiration probably does not affect the recovery factor by a large amount and that a value of $r \cong 0.9$ should suffice in design calculations.

In applying the results of this analysis as expressed in figures 8 and 9, it is convenient to express the parameter ζ in terms of the temperatures controlling a given cooling problem. If an effectiveness of cooling is defined by

$$E = \frac{T_e - T_W}{T_e - T_c} \tag{12}$$

for a surface where a heat balance (eq. (9)) applies, it is possible to relate ζ and E by

$$E = \frac{\zeta}{\zeta + \frac{St}{(c_f/2)}} \tag{13}$$

Thus, once E is specified for a given design, it is possible to determine ζ and, consequently, c_f, St, and $\rho_W v_W$ for given flight conditions and surface temperature.

CONCLUDING REMARKS

It can be concluded from the results of the present analysis that a transpiration cooling system is highly effective, even at high flight speeds. Not only does the coolant absorb a maximum amount of heat by attaining as its end temperature the temperature of the surface that it is cooling, but it has the further advantage that the effect of the transpiration greatly reduces both the skin friction and the amount of heat entering the surface.

Ames Aeronautical Laboratory
National Advisory Committee for Aeronautics
Moffett Field, Calif., Aug. 12, 1954

APPENDIX A

DETAILS OF ANALYSIS

When it is assumed that changes in the x direction are negligible compared to changes in the y direction, equations (1) through (3) become

$$\frac{d}{dy}\left(\bar{\rho}\bar{v} + \overline{\rho'v'}\right) = 0 \tag{A1}$$

$$\left(\bar{\rho}\bar{v} + \overline{\rho'v'}\right)\frac{d\bar{u}}{dy} = \frac{d}{dy}\left(\mu\frac{d\bar{u}}{dy} - \bar{\rho}\overline{u'v'}\right) \tag{A2}$$

$$\left(\bar{\rho}\bar{v} + \overline{\rho'v'}\right)\frac{d}{dy}\left(c_p\bar{T} + \frac{\bar{u}^2}{2}\right) = \frac{d}{dy}\left(\bar{k}\frac{d\bar{T}}{dy} + \bar{\mu}\bar{u}\frac{d\bar{u}}{dy} - \bar{\rho}c_p\overline{v'T'} + \bar{u}\overline{\rho u'v'}\right) \tag{A3}$$

These equations can be simplified by integrating equation (A1). The integral of equation (A1) is

$$\bar{\rho}\bar{v} + \overline{\rho'v'} = \text{constant} \tag{A4}$$

At the surface of the plate

$$\bar{\rho}\bar{v} = \rho_w v_w \tag{A5}$$

and

$$\overline{\rho'v'} = 0 \tag{A6}$$

Therefore,

$$\bar{\rho}\bar{v} + \overline{\rho'v'} = \rho_w v_w \tag{A7}$$

Equations (A2) and (A3) thus become

$$\rho_w v_w\frac{d\bar{u}}{dy} = \frac{d}{dy}\left(\bar{\mu}\frac{d\bar{u}}{dy} - \bar{\rho}\overline{u'v'}\right) \tag{A8}$$

$$\rho_W v_W \frac{d}{dy}\left(c_p\bar{T} + \frac{\bar{u}^2}{2}\right) = \frac{d}{dy}\left(\bar{k}\frac{d\bar{T}}{dy} + \bar{\mu}\bar{u}\frac{d\bar{u}}{dy} - \bar{\rho}c_p\overline{v'T'} - \bar{u}\overline{\rho u'v'}\right) \quad (A9)$$

It is convenient, at this point, to introduce the concepts of eddy viscosity, eddy thermal conductivity, and turbulent Prandtl number. The eddy viscosity and eddy thermal conductivity are defined as:

$$\epsilon_M = \frac{-\bar{\rho}\overline{u'v'}}{\left(\frac{d\bar{u}}{dy}\right)} \quad (A10)$$

and

$$\epsilon_H = -\frac{\bar{\rho}c_p\overline{v'T'}}{\left(\frac{d\bar{T}}{dy}\right)} \quad (A11)$$

The usual definition of Prandtl number is $\mu c_p/k$, where the fluid properties are based on the molecular transport of momentum and energy. In this analysis there is also employed the analogous quantity $\epsilon_M c_p/\epsilon_H$ in which the properties, in effect, are based on the turbulent transport of momentum and energy. This quantity is called the turbulent Prandtl number and is given the symbol Pr_t.

When equations (A10) and (A11) are introduced into equations (A8) and (A9) there results

$$\rho_W v_W \frac{du}{dy} = \frac{d}{dy}\left[(\mu + \epsilon_M)\frac{du}{dy}\right] \quad (A12)$$

$$\rho_W v_W \frac{d}{dy}\left(c_pT + \frac{u^2}{2}\right) = \frac{d}{dy}\left[\left(\frac{\mu}{Pr} + \frac{\epsilon_M}{Pr_t}\right)\frac{d}{dy}(c_pT) + (\mu + \epsilon_M)\frac{d\left(\frac{u^2}{2}\right)}{dy}\right] \quad (A13)$$

Note that the bars representing time-average quantities have been dropped in these equations as all the terms are mean values, the fluctuating terms no longer appearing.

I.- SKIN-FRICTION RELATIONSHIP FOR $Pr = Pr_t = 1$

Temperature-Velocity Relationship

For the case where $Pr = Pr_t = 1$, equation (A13) becomes

$$\rho_W v_W \frac{d}{dy}\left(c_p T + \frac{u^2}{2}\right) = \frac{d}{dy}\left[(\mu + \epsilon_M)\frac{d}{dy}\left(c_p T + \frac{u^2}{2}\right)\right] \tag{A14}$$

Equation (A14) has the identical form of equation (A12). Thus, if u is a solution of equation (A12), then

$$c_p T + \frac{u^2}{2} = au + b \tag{A15}$$

is a solution of (A14) since it is linear. The terms a and b are constants to be evaluated at the boundary conditions:

$$T = T_1 \quad \text{at} \quad u = u_1 \ (\text{outer edge})$$

$$T = T_W \quad \text{at} \quad u = 0 \ (\text{surface})$$

When these boundary conditions are employed, equation (A15) becomes

$$\frac{T}{T_W} = 1 + B\tilde{u} - A^2\tilde{u}^2 \tag{A16}$$

where

$$A^2 = \frac{\frac{\gamma - 1}{2} M_1^2}{\left(\frac{T_W}{T_1}\right)} \tag{A17}$$

$$B = \frac{1 + \frac{\gamma - 1}{2} M_1^2}{\left(\frac{T_W}{T_1}\right)} - 1 \tag{A18}$$

$$\tilde{u} = \frac{u}{u_1} \tag{A19}$$

Because of equation (A16), it is only necessary to integrate the momentum equation (A12) to obtain both the velocity and temperature distribution in the boundary layer. To perform this integration, it is assumed that the boundary layer is divided into two parts: a sublayer,

adjacent to the surface, where momentum transfer is by molecular means alone; and an outer portion of the boundary layer, where momentum transfer is by eddying motion alone.

Velocity Distribution in the Sublayer

In the sublayer, equation (A12) is written as

$$\rho_W v_W \frac{du}{dy} = \frac{d}{dy}\left(\mu \frac{du}{dy}\right) \tag{A20}$$

Since $\rho_W v_W$ is not a function of y, equation (A20) can be integrated directly to yield

$$\rho_W v_W u = \mu \frac{du}{dy} + \text{constant} \tag{A21}$$

The constant in equation (A21) can be evaluated by employing the boundary conditions

$$y = 0 \qquad u = 0 \qquad \tau_W = \mu \frac{du}{dy} \tag{A22}$$

Equation (A21) becomes

$$\mu \frac{du}{dy} = \tau_W + \rho_W v_W u \tag{A23}$$

Integration of equation (A23) yields

$$y = \int_0^u \frac{\mu du}{\rho_W v_W u + \tau_W} \tag{A24}$$

It was shown in the Discussion that the extent of the sublayer under the conditions of blowing is not well known. In view of this, extreme rigor in the integration of the right member of equation (A24) is not mandatory. For simplicity, then, let $\mu = \mu_W$ and the resulting integration yields

$$y^+ = \frac{\sqrt{\frac{c_f}{2}}\left(\frac{T_W}{T_1}\right)^{\omega}}{\frac{\rho_W v_W}{\rho_1 u_1}} \ln\left(1 + \frac{\rho_W v_W}{\rho_1 u_1} \frac{u^+}{\sqrt{\frac{c_f}{2}}}\right) \tag{A25}$$

where

$$y^+ = \frac{\rho_1 u_1 \sqrt{\frac{c_f}{2}}\, y}{\mu_1} \tag{A26}$$

$$u^+ = \frac{\tilde{u}}{\sqrt{\frac{c_f}{2}}} \tag{A27}$$

$$\frac{\mu_1}{\mu_W} = \left(\frac{T_1}{T_W}\right)^{\omega} \tag{A28}$$

Velocity Distribution in the Outer Turbulent Portion

In the outer turbulent portion, equation (A12) is written as

$$\rho_W v_W \frac{du}{dy} = \frac{d}{dy}\left(\epsilon_M \frac{du}{dy}\right) \tag{A29}$$

By employing Prandtl's mixing-length concepts $\epsilon_M = \rho l^2 \left(\frac{du}{dy}\right)$ and using $l = Ky$, equation (A29) can be rewritten in the form

$$\rho_W v_W \frac{du}{dy} = \frac{d}{dy}\left[\rho K^2 y^2 \left(\frac{du}{dy}\right)^2\right] \tag{A30}$$

Because $\rho_W v_W$ is not a function of y, equation (A30) can be integrated directly to yield

$$\rho_W v_W u = \rho K^2 y^2 \left(\frac{du}{dy}\right)^2 + \text{constant} \tag{A31}$$

At the interface of the sublayer and outer turbulent portion, it is required that the velocity on the laminar side match the velocity on the turbulent side. In addition, a matching of the laminar and turbulent shears is also required. By comparison of corresponding terms of equations (A21) and (A31), it is apparent that the matching of the velocities

and shears requires the constants to be the same. Thus, equation (A31) can be rewritten as

$$\rho_W v_W u + \tau_W = \rho K^2 y^2 \left(\frac{du}{dy}\right)^2 \tag{A32}$$

Integration of equation (A32) results in

$$y = y_a \exp \int_{u_a}^{u} \frac{K\rho^{1/2}\, du}{\sqrt{\rho_W v_W u + \tau_W}} \tag{A33}$$

It will be convenient later to represent the exponential term in equation (A33) by the symbol g, thus

$$y = y_a\, g \tag{A34}$$

Because the primary concern of this analysis is the determination of skin friction and heat transfer at the surface, it is not necessary to perform the integration indicated in equation (A33) at this stage of the analysis.

Substitution of Velocity Distribution Into von Kármán Momentum Equation

The von Kármán momentum-integral equation for the case with surface blowing at constant pressure can be written as

$$\tau_W + \rho_W v_W u_1 = \frac{d}{dx}\int_0^{\delta} \rho u\,(u_1 - u)\, dy \tag{A35}$$

Equation (A35) can be made dimensionless by dividing through by $\rho_1 u_1^2$. It is also convenient to replace the variable of integration y by $\tilde{u}$. The resulting equation is

$$\frac{c_f}{2} + \frac{\rho_W v_W}{\rho_1 u_1} = \frac{d}{dx}\int_0^1 \left(\frac{\rho}{\rho_1}\right) \tilde{u}\,(1 - \tilde{u}) \left(\frac{dy}{d\tilde{u}}\right) d\tilde{u} \tag{A36}$$

The integral in the term on the right represents the momentum thickness θ.

To evaluate the momentum thickness rigorously in equation (A36), it would be necessary to divide it into two parts. The first part, with the lower bound as 0 and the upper bound as $\tilde{u}_a$, would represent the contribution of the sublayer. The second part, with the lower bound as $\tilde{u}_a$ and the upper bound as 1, would represent the contribution of the outer turbulent portion. In the first part $(dy/d\tilde{u})$ would be evaluated from equation (A23), while in the second part it would be evaluated from equation (A33). For the incompressible case without blowing, these integrations can be performed very simply in closed form. It is found that this two-part system can be approximated very closely (less than 1-percent difference in $c_f(R_\theta)$ curves) by the integral of the second part in which the lower bound is set equal to zero. It would not be expected that the introduction of compressibility and blowing should markedly alter this behavior; consequently, the simpler one-part system will be used in the present analysis to determine θ.

When $(dy/d\tilde{u})$ is evaluated from equation (A33), the expression for momentum thickness becomes

$$\theta = Ky_a \int_0^1 \left(\frac{\rho}{\rho_1}\right)^{3/2} \tilde{u}(1-\tilde{u}) \frac{g}{\sqrt{\frac{\rho_w v_w}{\rho_1 u_1}\tilde{u} + \frac{c_f}{2}}}\, d\tilde{u} \tag{A37}$$

noting that

$$g = \exp \int_{\tilde{u}_a}^{\tilde{u}} \frac{K\left(\frac{\rho}{\rho_1}\right)^{1/2} d\tilde{u}}{\sqrt{\frac{\rho_w v_w}{\rho_1 u_1}\tilde{u} + \frac{c_f}{2}}} \tag{A38}$$

Equation (A37) cannot be solved in closed form; however, if the condition of compressibility is removed, a closed form solution for θ can be obtained easily. It is found from the solution for the incompressible case that the first term resulting from an integration by parts yields results which have the same form as the results of the complete integration. Since we are primarily concerned with the form of the solution, absolute magnitudes can be adjusted by slight changes in u_a^+ and K which are arbitrary constants; only the first term resulting from an integration by parts of the compressible case will be used in this analysis.

To perform the integration of equation (A37), it is necessary to replace $\tilde{u}$ as the variable of integration by g. From equation (A38)

$$dg = \frac{K\left(\frac{\rho}{\rho_1}\right)^{1/2}}{\sqrt{\frac{\rho_w v_w}{\rho_1 u_1}\tilde{u} + \frac{c_f}{2}}}\, g\, d\tilde{u} \tag{A39}$$

Substitution of equation (A39) into equation (A37) yields

$$\theta = y_a \int_{g(o)}^{g(1)} \left(\frac{\rho}{\rho_1}\right) \tilde{u}\,(1-\tilde{u})\,dg \tag{A40}$$

Because the pressure across the boundary is assumed to be constant, the perfect gas law and equation (A16) indicate that

$$\frac{\rho}{\rho_1} = \left(\frac{T}{T_1}\right)^{-1} = \left(\frac{T_1}{T_W}\right)(1+B\tilde{u}-A^2\tilde{u}^2)^{-1} \tag{A41}$$

Equation (A40) then becomes

$$\theta = y_a \left(\frac{T_1}{T_W}\right) \int_{g(o)}^{g(1)} \frac{\tilde{u}(1-\tilde{u})\,dg}{1+B\tilde{u}-A^2\tilde{u}^2} \tag{A42}$$

When equation (A42) is integrated by parts, there results

$$\theta = y_a \left(\frac{T_1}{T_W}\right) \left[\frac{\tilde{u}(1-\tilde{u})g}{1+B\tilde{u}-A^2\tilde{u}^2}\Bigg|_{\tilde{u}=o}^{\tilde{u}=1} - \int_o^1 g\,\frac{1-2\tilde{u}+(A^2-B)\tilde{u}^2}{(1+B\tilde{u}-A^2\tilde{u}^2)^2}\,d\tilde{u} \right] \tag{A43}$$

From an examination of equation (A38) it is apparent that both $g(1)$ and $g(0)$ are finite; consequently, the first term on the right of equation (A43) vanishes at the bounds. If g is again substituted for $\tilde{u}$ as the variable of integration, equation (A43) becomes

$$\theta = -\frac{y_a \left(\frac{T_1}{T_W}\right)^{1/2}}{K} \int_{g(o)}^{g(1)} \frac{\left[1-2\tilde{u}+(A^2-B)\tilde{u}^2\right]\sqrt{\frac{\rho_W v_W}{\rho_1 u_1}\,\tilde{u}+\frac{c_f}{2}}}{(1+B\tilde{u}-A^2\tilde{u}^2)^{3/2}}\,dg \tag{A44}$$

Again, integrating by parts results in

$$\theta = -\frac{y_a \left(\frac{T_1}{T_W}\right)^{1/2}}{K} \left\{ \frac{\left[1-2\tilde{u}+(A^2-B)\tilde{u}^2\right]\sqrt{\frac{\rho_W v_W}{\rho_1 u_1}\,\tilde{u}+\frac{c_f}{2}}}{(1+B\tilde{u}-A^2\tilde{u}^2)^{3/2}}\, g \Bigg|_{\tilde{u}=o}^{\tilde{u}=1} + \text{additional terms} \right\} \tag{A45}$$

When the additional terms are omitted and the limits of integration are introduced

$$\theta = \frac{y_a \left(\frac{T_1}{T_W}\right)^{1/2}}{K} \left[\frac{g(1) \sqrt{\frac{c_f}{2} + \frac{\rho_W v_W}{\rho_1 u_1}}}{(1+B-A^2)^{1/2}} + g(0) \sqrt{\frac{c_f}{2}} \right] \tag{A46}$$

For practical cases $g(1) \gg g(0)$; therefore,

$$\theta = \frac{y_a \left(\frac{T_1}{T_W}\right)^{1/2}}{K} \frac{\sqrt{\frac{c_f}{2} + \frac{\rho_W v_W}{\rho_1 u_1}}}{(1+B-A^2)^{1/2}} g(1) \tag{A47}$$

But $\frac{T_1}{T_W} = (1+B-A^2)$, so that

$$\theta = \frac{y_a}{K} \sqrt{\frac{c_f}{2} + \left(\frac{\rho_W v_W}{\rho_1 u_1}\right)}\, g(1) \tag{A48}$$

Employing equation (A26)

$$R_\theta = \frac{y_a^+}{K} \sqrt{1 + \frac{\left(\frac{\rho_W v_W}{\rho_1 u_1}\right)}{\left(\frac{c_f}{2}\right)}}\, g(1) \tag{A49}$$

Equation (A49) can be manipulated into the form

$$\ln \frac{R_\theta K}{y_a^+ \sqrt{1 + \frac{\left(\frac{\rho_W v_W}{\rho_1 u_1}\right)}{(c_f/2)}}} = \int_{\tilde{u}_a}^{1} \frac{K \left(\frac{\rho}{\rho_1}\right)^{1/2} d\tilde{u}}{\sqrt{\frac{\rho_W v_W}{\rho_1 u_1} \tilde{u} + \frac{c_f}{2}}} \tag{A50}$$

Before integrating the right member of (A50), it is preferable to obtain the relationship of c_f in terms of the length Reynolds number.

Equation (A36) can be rewritten as

$$\frac{c_f}{2} + \frac{\rho_W v_W}{\rho_1 u_1} = \frac{d}{dR_x}\left(\frac{y_a^+}{K}\sqrt{1 + \frac{\left(\frac{\rho_W v_W}{\rho_1 u_1}\right)}{\frac{c_f}{2}}}\; g(1)\right) \tag{A51}$$

when equation (A49) is employed. On integration, neglecting the effect of laminar sublayer

$$R_x = \int_{\frac{c_f}{2} \to \infty}^{\frac{c_f}{2}(x)} \frac{d\left(\frac{y_a^+}{K}\sqrt{1 + \frac{(\rho_W v_W/\rho_1 u_1)}{(c_f/2)}}\; g(1)\right)}{\left(\frac{c_f}{2} + \frac{\rho_W v_W}{\rho_1 u_1}\right)} \tag{A52}$$

Integration by parts yields

$$R_x = \left.\frac{\frac{y_a^+}{K}\sqrt{1 + \frac{(\rho_W v_W/\rho_1 u_1)}{(c_f/2)}}\; g(1)}{(c_f/2) + (\rho_W v_W/\rho_1 u_1)}\right|_{\frac{c_f}{2} \to \infty}^{\frac{c_f}{2}(x)} + \text{additional terms} \tag{A53}$$

For large values of R_x the first term predominates. Also $g(1)$ is finite; therefore,

$$R_x = \frac{y_a^+}{K}\frac{g(1)}{\sqrt{\frac{c_f}{2}\left(\frac{c_f}{2} + \frac{\rho_W v_W}{\rho_1 u_1}\right)}} \tag{A54}$$

or

$$\ln \frac{K}{y_a^+}\sqrt{\frac{c_f}{2}\left(\frac{c_f}{2} + \frac{\rho_W v_W}{\rho_1 u_1}\right)}\; R_x = \int_{\tilde{u}_a}^{1} \frac{K\left(\frac{\rho}{\rho_1}\right)^{1/2} d\tilde{u}}{\sqrt{\frac{\rho_W v_W}{\rho_1 u_1}\tilde{u} + \frac{c_f}{2}}} \tag{A55}$$

It is apparent that the right members of equations (A50) and (A55) are identical. This does not mean that the left members are equal, but just that the K and u_a^+ (also y_a^+) used in each of the equations are different (see Discussion)

The integral appearing in equations (A50) and (A55) can be written as

$$K\left(\frac{T_1}{T_W}\right)^{1/2} \int_{\tilde{u}_a}^{1} \frac{d\tilde{u}}{\sqrt{\frac{\rho_W v_W}{\rho_1 u_1}\tilde{u} + \frac{c_f}{2}}\sqrt{1+B\tilde{u}-A^2\tilde{u}^2}} \tag{A56}$$

when equation (A16) is employed. The integral (A56) can be rewritten as

$$\frac{K\left(\frac{T_1}{T_W}\right)^{1/2}}{A\sqrt{\frac{\rho_W v_W}{\rho_1 u_1}}} \int_{\tilde{u}_a}^{1} \frac{d\tilde{u}}{\sqrt{(\tilde{u}+\sigma)(\tilde{u}-\alpha)(\beta-\tilde{u})}} \tag{A57}$$

where

$$\alpha = \frac{B - \sqrt{B^2+4A^2}}{2A^2} \tag{A58}$$

$$\beta = \frac{B + \sqrt{B^2+4A^2}}{2A^2} \tag{A59}$$

$$\sigma = \frac{(c_f/2)}{\left(\frac{\rho_W v_W}{\rho_1 u_1}\right)} \tag{A60}$$

Letting

$$\sin^2 \varphi = c\,(\beta-\tilde{u}) \tag{A61}$$

then $d\tilde{u} = -\frac{2}{c}\sin\varphi\cos\varphi\,d\varphi$ and the integral (A57), on transforming the variable of integration from $\tilde{u}$ to φ, becomes

$$-\frac{2K\left(\frac{T_1}{T_W}\right)^{1/2}}{A\sqrt{\frac{\rho_W v_W}{\rho_1 u_1}}} \int_{\varphi(\tilde{u}_a)}^{\varphi(1)} \frac{\frac{1}{\sqrt{c}}\cos\varphi\,d\varphi}{\sqrt{\left[(\beta+\sigma) - \frac{1}{c}\sin^2\varphi\right]\left[(\beta-\alpha) - \frac{1}{c}\sin^2\varphi\right]}} \tag{A62}$$

If c is set equal to $\frac{1}{\beta+\sigma}$ then integral (A62) becomes

$$-\frac{2K\left(\frac{T_1}{T_W}\right)^{1/2}}{A\sqrt{\frac{\rho_W v_W}{\rho_1 u_1}}\sqrt{\beta-\alpha}}\int_{\varphi(\tilde{u}_a)}^{\varphi(1)}\frac{d\varphi}{\sqrt{1-\frac{\beta+\sigma}{\beta-\alpha}\sin^2\varphi}} \tag{A63}$$

Since Legendre's standard form of the elliptic integral of the first kind is

$$F(k,\varphi)=\int_0^{\varphi}\frac{d\varphi}{\sqrt{1-k^2\sin^2\varphi}} \tag{A64}$$

Integral (A63) can be rewritten as

$$\frac{2K\left(\frac{T_1}{T_W}\right)^{1/2}}{A\sqrt{\frac{\rho_W v_W}{\rho_1 u_1}}\sqrt{\beta-\alpha}}\left\{F\left[k_m,\varphi_m(\tilde{u}_a)\right]-F\left[k_m,\varphi(1)\right]\right\} \tag{A65}$$

where

$$\left.\begin{aligned} k_m^2&=\frac{\beta+\sigma}{\beta-\alpha}<1\\ \text{and}\qquad \sin^2\varphi_m(\tilde{u})&=\frac{\beta-\tilde{u}}{\beta+\sigma}\end{aligned}\right\} \tag{A66}$$

If c in equation (A62) is set equal to $1/\beta-\alpha$, integral (A63) becomes

$$\frac{2K\left(\frac{T_1}{T_W}\right)^{1/2}}{A\sqrt{\frac{\rho_W v_W}{\rho_1 u_1}}\sqrt{\beta+\sigma}}\left\{F\left[k_n,\varphi_n(\tilde{u}_a)\right]-F\left[k_n,\varphi_n(1)\right]\right\} \tag{A67}$$

where

$$\left.\begin{aligned} k_n^2&=\frac{\beta-\alpha}{\beta+\sigma}<1\\ \sin^2\varphi_n(\tilde{u})&=\frac{\beta-\tilde{u}}{\beta-\alpha}\end{aligned}\right\} \tag{A68}$$

II.- SKIN FRICTION - HEAT TRANSFER RELATIONSHIP FOR $Pr \neq 1$.

This part of the analysis begins with the integration of equations (A12) and (A13), resulting in

$$\rho_W v_W u = (\mu + \epsilon_M) \frac{du}{dy} + c_1 \tag{A69}$$

and

$$\rho_W v_W \left(c_p T + \frac{u^2}{2}\right) = \left(\frac{\mu}{Pr} + \frac{\epsilon_M}{Pr_t}\right) \frac{dc_p T}{dy} + (\mu+\epsilon_M) \frac{d\left(\frac{u^2}{2}\right)}{dy} + c_2 \tag{A70}$$

where c_1 and c_2 are arbitrary constants. At the surface $y = 0$, we have

$$U = 0 \qquad \epsilon_M = 0$$

$$T = T_W$$

$$\tau_W = \mu \frac{du}{dy}\bigg|_W$$

$$q_W = - k \frac{dT}{dy}\bigg|_W = - \frac{\mu}{Pr} \frac{dc_p T}{dy}\bigg|_W$$

At the surface, equations (A69) and (A70) thus become

$$0 = \tau_W + c_1 \tag{A71}$$

$$\rho_W v_W c_p T_W = - q_W + c_2 \tag{A72}$$

When the arbitrary constants evaluated from equations (A71) and (A72) are substituted into equations (A69) and (A70), there results

$$\rho_W v_W u + \tau_W = (\mu + \epsilon_M) \frac{du}{dy} \tag{A73}$$

$$\rho_W v_W \left[c_p (T - T_W) + \frac{u^2}{2} \right] - q_W = \left(\frac{\mu}{Pr} + \frac{\epsilon_M}{Pr_t}\right) \frac{dc_p T}{dy} + (\mu+\epsilon_M) u \frac{du}{dy} \tag{A74}$$

Dividing the terms of equation (A74) by the terms of equation (A73) yields

$$\frac{\rho_W v_W \left[c_p(T-T_W) + \frac{u^2}{2}\right] - q_W}{\rho_W v_W u + \tau_W} = \frac{\left(\frac{\mu}{Pr} + \frac{\epsilon_M}{Pr_t}\right)}{(\mu + \epsilon_M)} \frac{dc_pT}{du} + u \tag{A75}$$

It is convenient in the processes which follow to introduce the following symbols:

$$P = \frac{(\mu + \epsilon_M)}{\left(\frac{\mu}{Pr} + \frac{\epsilon_M}{Pr_t}\right)} \qquad F = \frac{\rho_W v_W}{\rho_1 u_1}$$

$$S = \frac{q_W}{\rho_1 u_1} \qquad E = c_p(T-T_W) + \frac{u^2}{2}$$

Equation (A75) can then be written as

$$\frac{dE}{d\tilde{u}} - \frac{PF}{F\tilde{u} + c_f/2} E = (1-P) u_1^2 \tilde{u} - \frac{PS}{F\tilde{u} + c_f/2} \tag{A76}$$

In the range $0 < \tilde{u} < \tilde{u}_a$ $\quad P = Pr$

$\tilde{u}_a < \tilde{u} < 1$ $\quad P = Pr_t$

Equation (A76) must then be integrated in two stages with the results combined at the interface where $\tilde{u} = \tilde{u}_a$. The integration, with the use of an integrating factor, is straightforward. After some algebraic manipulation, there results back in the original notation

$$\frac{q_W}{\rho_1 u_1} = \frac{\left(c_pT_W - c_pT_1 - r\frac{u_1^2}{2}\right)\frac{\rho_W v_W}{\rho_1 u_1}}{\left(\frac{c_f}{2}\right)^{-Pr}\left(\frac{\rho_W v_W}{\rho_1 u_1}\tilde{u}_a + \frac{c_f}{2}\right)^{Pr-Pr_t}\left(\frac{\rho_W v_W}{\rho_1 u_1} + \frac{c_f}{2}\right)^{Pr_t} - 1} \tag{A77}$$

If we define the heat-transfer coefficient as

$$h = \frac{q_W}{T_W - T_1 - r\frac{u_1^2}{2c_p}} \tag{A78}$$

the final relationship relating heat transfer and skin friction is

$$\frac{St}{\frac{c_f}{2}} = \frac{\left(\frac{\rho_W v_W}{\rho_1 u_1}\right)}{\left(\frac{c_f}{2}\right)^{1-Pr}\left(\frac{\rho_W v_W}{\rho_1 u_1}\tilde{u}_a + \frac{c_f}{2}\right)^{Pr-Pr_t}\left(\frac{\rho_W v_W}{\rho_1 u_1} + \frac{c_f}{2}\right)^{Pr_t} - \frac{c_f}{2}} \tag{A79}$$

The expression defining the recovery factor is

$$r = 1 - 2\frac{\left(\frac{\rho_W v_W}{\rho_1 u_1}\right)\left(\frac{\rho_W v_W}{\rho_1 u_1} + \frac{c_f}{2}\right)(2-Pr)(2-Pr_t) - (2-Pr)\left(\frac{\rho_W v_W}{\rho_1 u_1} + \frac{c_f}{2}\right)^2 + \left(\frac{\rho_W v_W}{\rho_1 u_1}\tilde{u}_a + \frac{c_f}{2}\right)^{2-Pr_t}\left(\frac{\rho_W v_W}{\rho_1 u_1} + \frac{c_f}{2}\right)^{Pr_t}(Pr_t - Pr)}{\left(\frac{\rho_W v_W}{\rho_1 u_1}\right)^2(2 - Pr_t)(2 - Pr)}$$

$$- 2\frac{(2 - Pr_t)\left(\frac{c_f}{2}\right)^{2-Pr}\left(\frac{\rho_W v_W}{\rho_1 u_1}\tilde{u}_a + \frac{c_f}{2}\right)^{Pr-Pr_t}\left(\frac{\rho_W v_W}{\rho_1 u_1} + \frac{c_f}{2}\right)^{Pr_t}}{\left(\frac{\rho_W v_W}{\rho_1 u_1}\right)^2(2 - Pr_t)(2 - Pr)} \tag{A80}$$

REFERENCES

1. Eckert, E. R. G., and Livingood, John N. B.: Comparison of Effectiveness of Convection-, Transpiration-, and Film-Cooling Methods With Air as Coolant. NACA TN 3010, 1953.

2. Eckert, E. R. G.: Heat Transfer and Temperature Profiles in Laminar Boundary Layers on a Sweat-Cooled Wall. AAF, Air Materiel Command, Wright Field. TR 5646, 1947.

3. Brown, W. Byron, and Donoughe, Patrick L.: Tables of Exact Laminar-Boundary-Layer Solutions when the Wall is Porous and Fluid Properties are Variable. NACA TN 2479, 1951.

4. Rannie, W. D.: A Simplified Theory of Porous Wall Cooling. (Progress rept. 4-50. ORDCIT proj. Contract W-04-200-ORD-455, Ordnance Dept. Power Plant Lab. proj. MX801, Contract W-535-AC-20260, Air Mat. Com.) C.I.T., Pasadena (Guggenheim Aero. Lab.), Jet Propulsion Lab.

5. Friedman, Joseph: A Theoretical and Experimental Investigation of Rocket-Motor Sweat Cooling. Jour. American Rocket Soc., No. 79, December 1949, pp. 147-154.

6. Crocco, L.: An Approximate Theory of Porous, Sweat, or Film Cooling With Reactive Fluids. Jour. American Rocket Soc., vol. 22, no. 6, Nov.-Dec. 1952, pp. 331-338.

7. Duwez, P., and Wheeler, H. L.: Experimental Study of Cooling by Injection of a Fluid Through a Porous Material. Jour. Aero. Sci., vol. 15, no. 9, Sept. 1948, pp. 509-521.

8. Jakob, M., and Fieldhouse, I. B.: Cooling by Forcing a Fluid Through a Porous Plate in Contact With a Hot Gas Stream. Heat Transfer and Fluid Mech. Inst. (Paper presented at June 22-24, 1949 meeting) A.S.M.E.

9. Mickley, H. S., Ross, R. C., Squyers, A. L., and Stewart, W. E.: Heat, Mass, and Momentum Transfer for Flow Over a Flat Plat With Blowing or Suction. M.I.T., Sept. 1952, NACA Contract NAw 5980.

10. Rubesin, Morris W.: A Modified Reynolds Analogy for the Compressible Turbulent Boundary Layer on a Flat Plate. NACA TN 2917, 1953.

11. Li, Ting-Yi, and Nagamatsu, H. T.: Effect of Density Fluctuations on the Turbulent Skin Friction on a Flat Plate at High Supersonic Speeds. Proc. of the Second Midwestern Conference on Fluid Mechanics, 1952. Ohio State Univ. Engineering Experiment Station Bulletin No. 149, pp. 263-275.

12. Coles, Donald: Measurements in the Boundary Layer on a Smooth Flat Plate in Supersonic Flow. C.I.T. Thesis, Pasadena, California, 1953.

13. McAdams, William Henry: Heat Transmission. McGraw-Hill, New York, 1942, p. 175.

14. Fage, A., and Falkner, V. M.: Relation Between Heat Transfer and Surface Friction for Laminar Flow. R. & M. No. 1408, British A.R.C., 1931.

15. Colburn, Allan Philip: A Method of Correlating Forced Convection Heat Transfer Data and a Comparison With Fluid Friction. Trans. Am. Inst. Chem. Engr., vol. 29, 1933, pp. 174-210.

16. Rubesin, Morris W.: The Effect of an Arbitrary Surface-Temperature Variation Along a Flat Plate on the Convective Heat Transfer in an Incompressible Turbulent Boundary Layer. NACA TN 2345, April 1951.

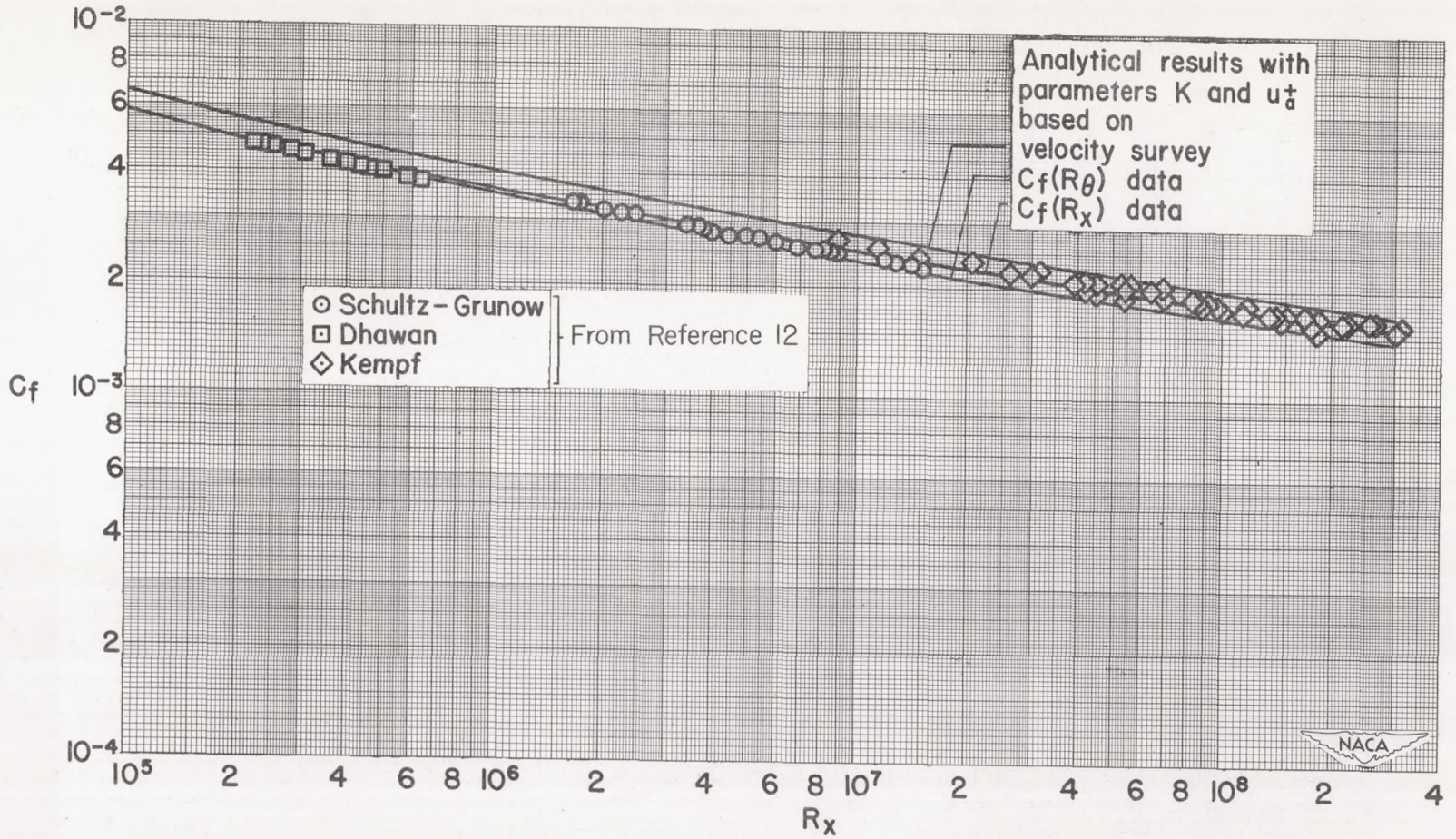

Figure 1.- Direct measurements of local skin friction in low-speed flow compared with analytical results based on alternative choices of arbitrary parameters.

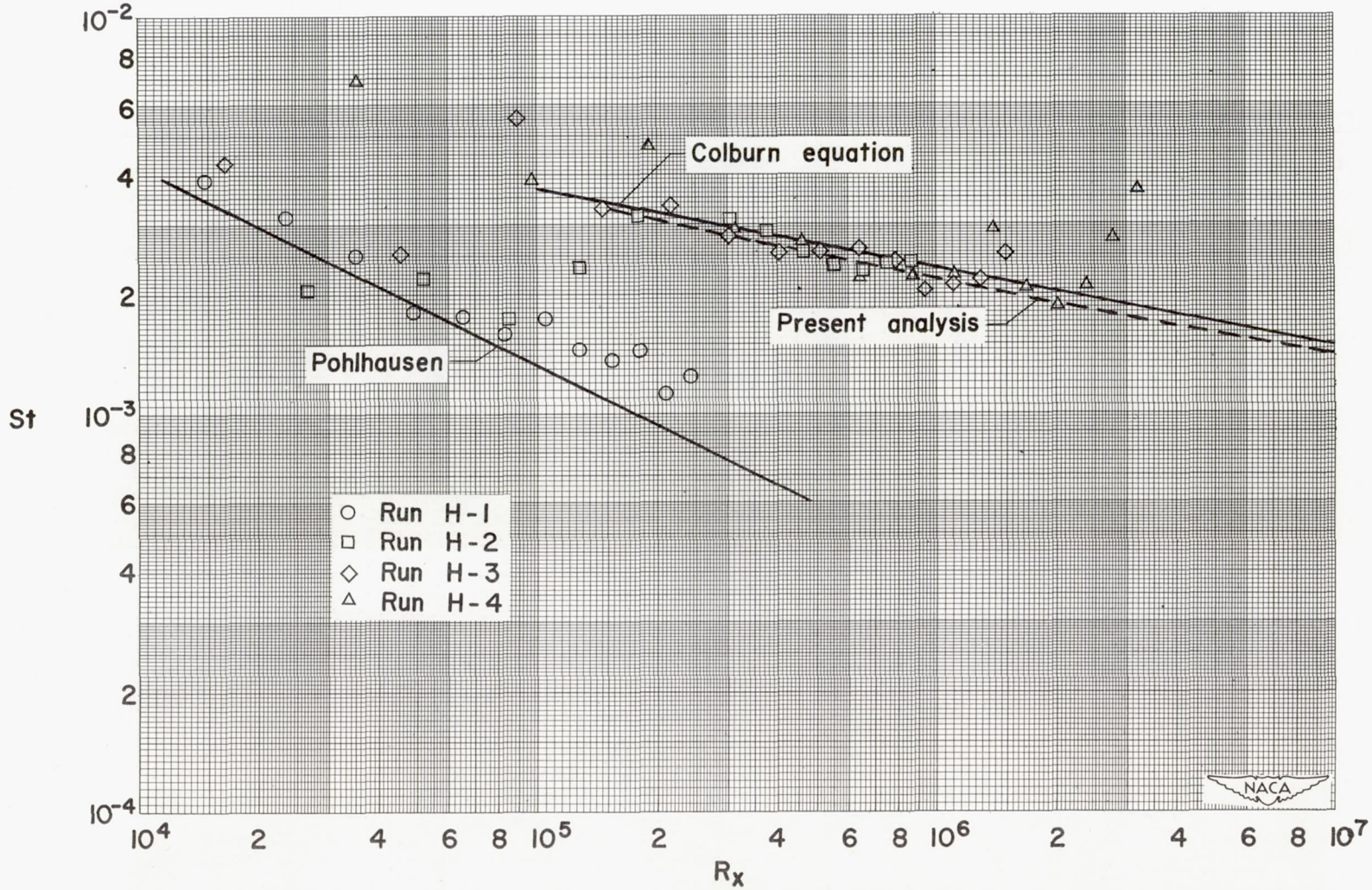

Figure 2.- Data of reference 9 for incompressible flow, no transpiration case compared with results of present analysis.

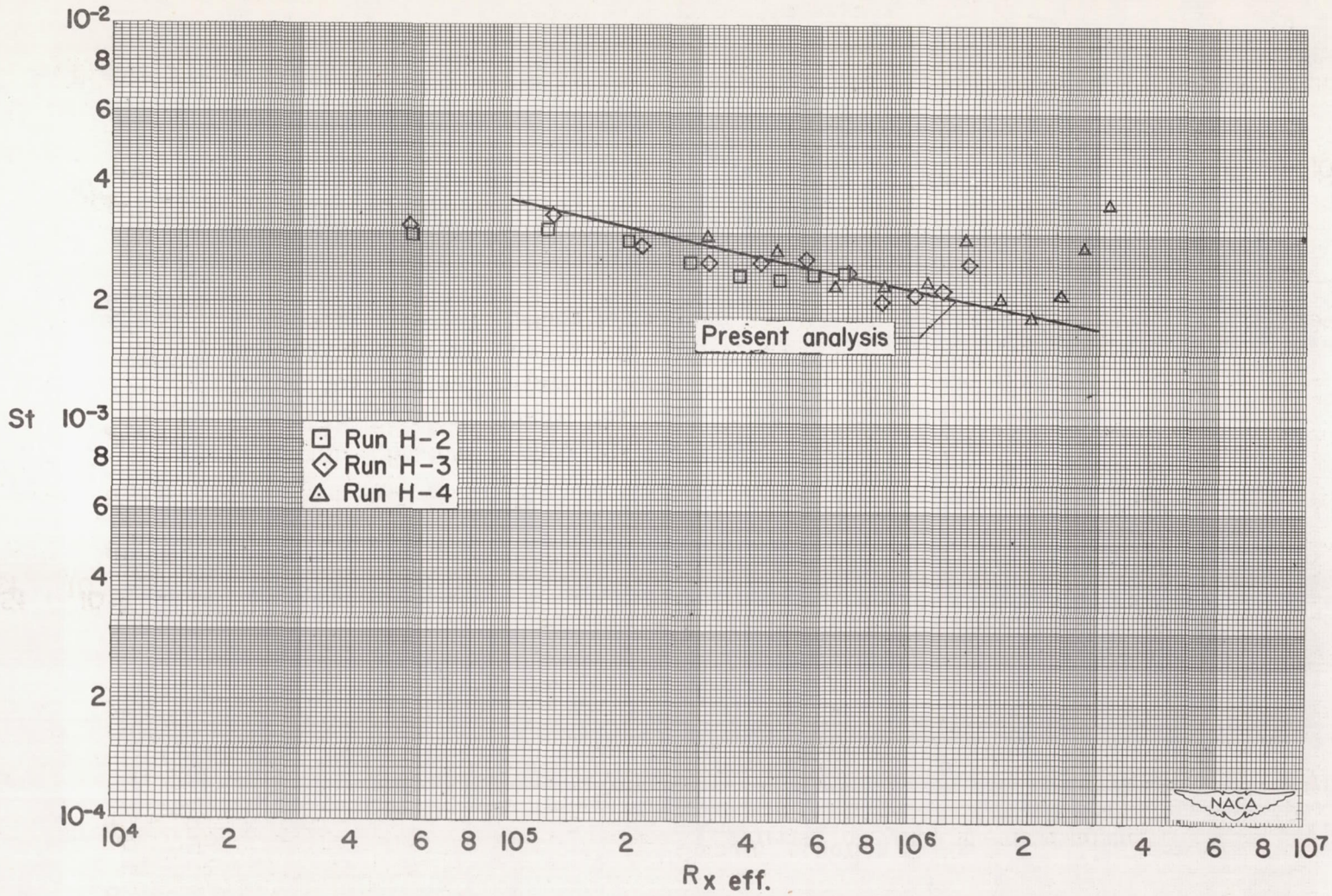

Figure 3.- Data of figure 2 overcorrected for effective length Reynolds number.

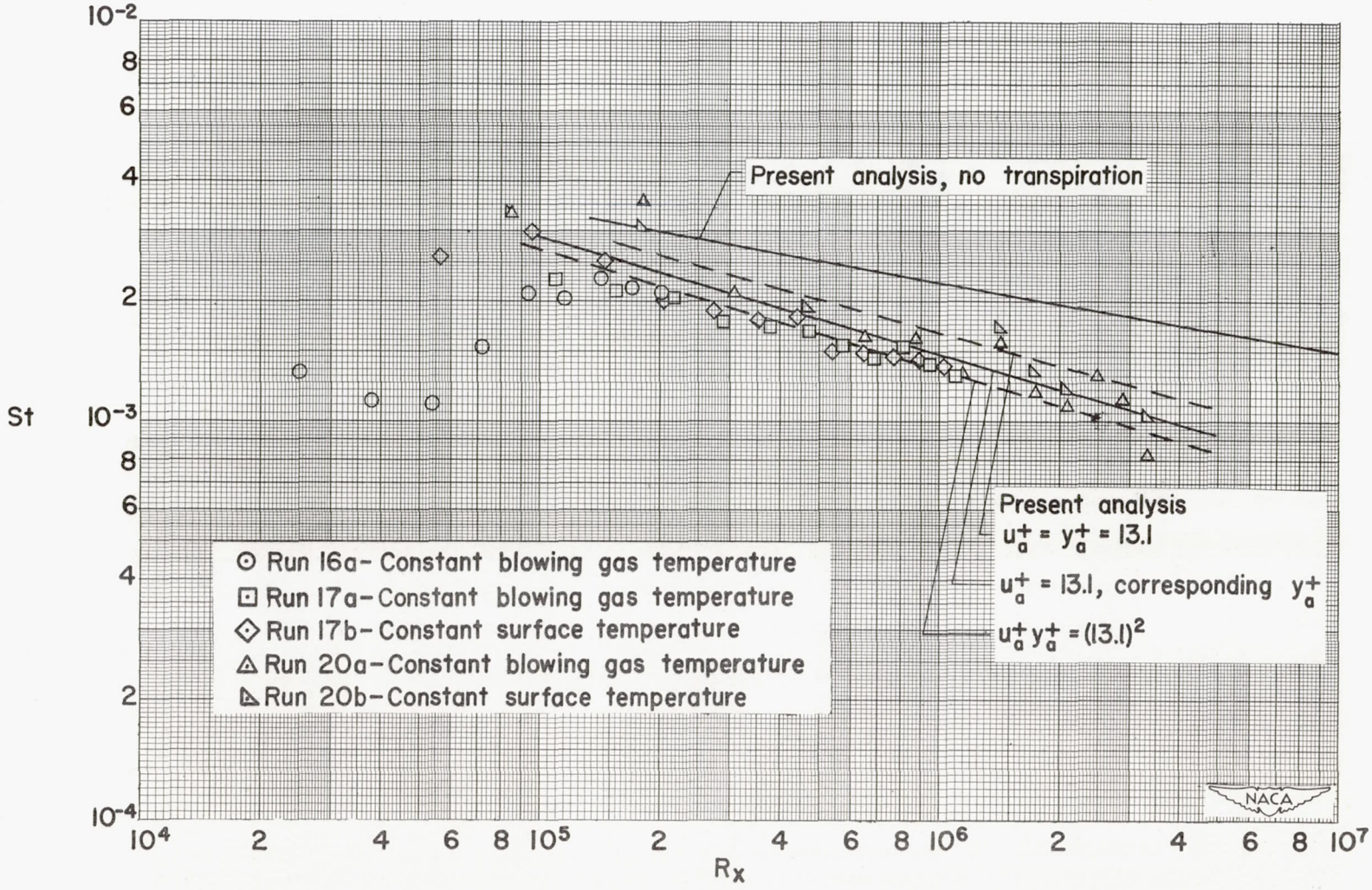

Figure 4.- Data of reference 9 for incompressible flow with uniform transpiration $\frac{\rho_w v_w}{\rho_1 u_1} = 0.002$ compared with present analysis.

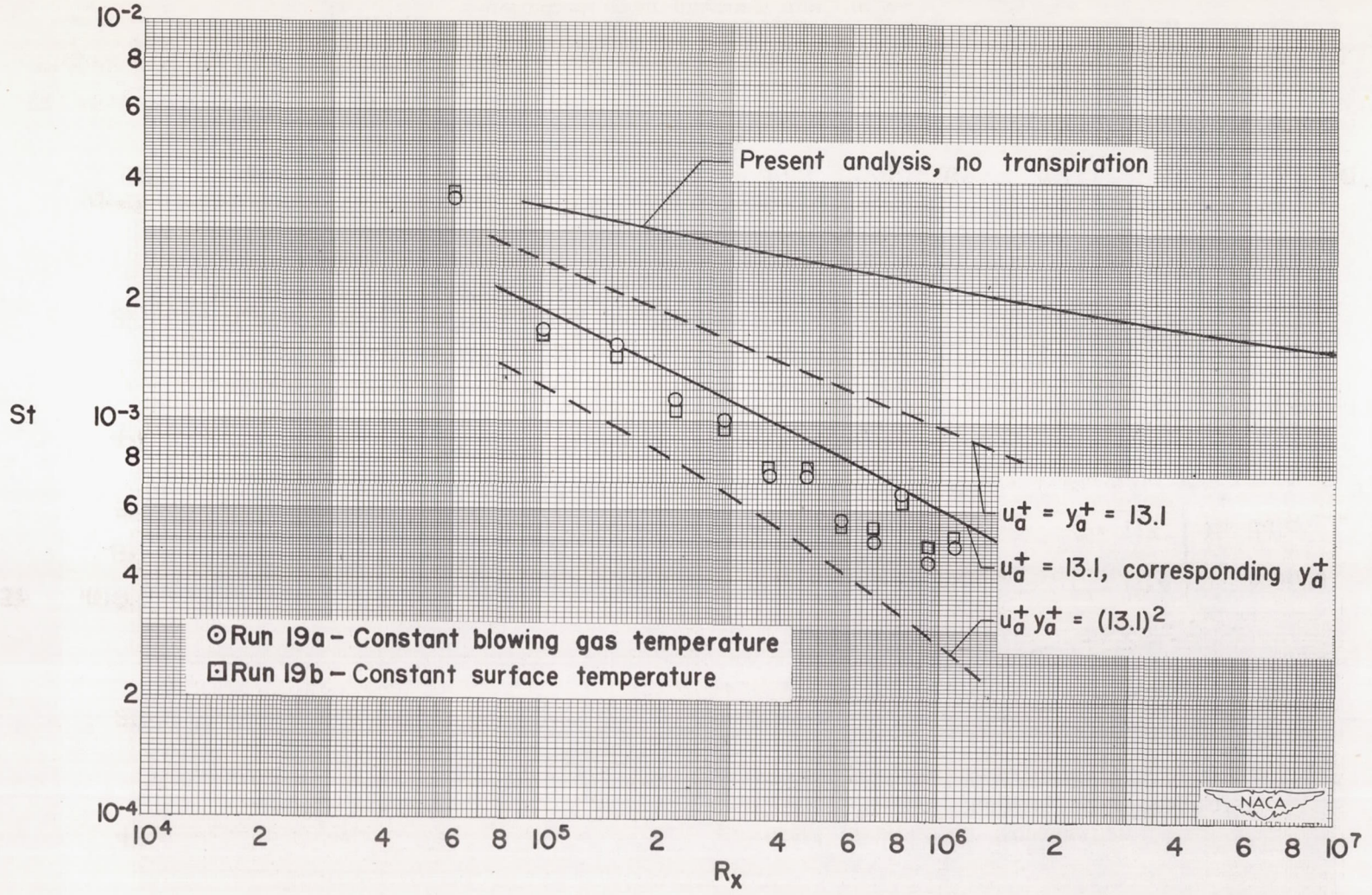

Figure 5.- Data of reference 9 for incompressible flow with uniform transpiration $\frac{\rho_w v_w}{\rho_1 u_1} = 0.006$ compared with present analysis.

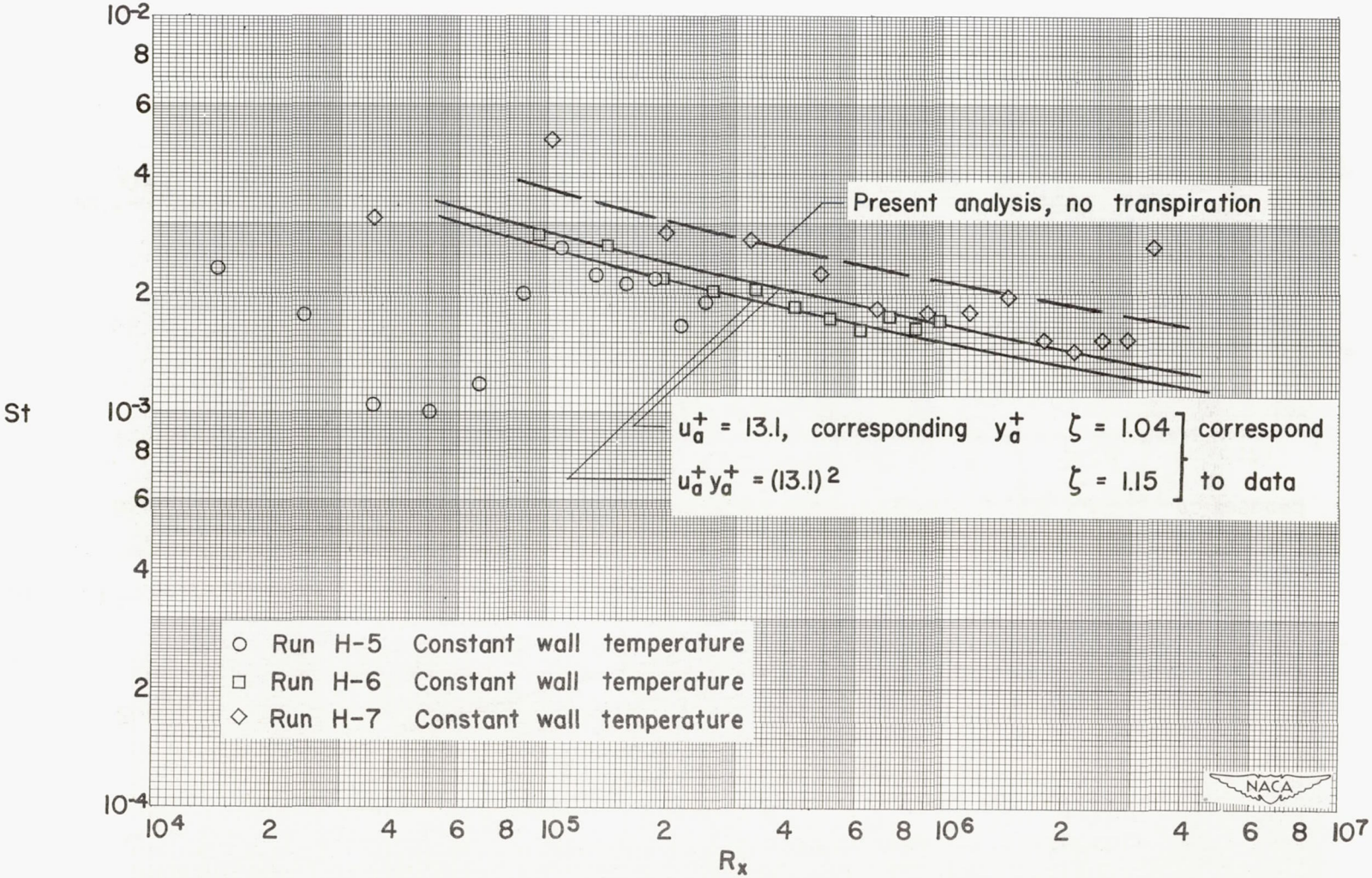

Figure 6.- Data of reference 9 for incompressible flow with varying transpiration rate $\frac{\rho_w v_w}{\rho_1 u_1} = \zeta\left(\frac{c_f}{2}\right)$ compared with present analysis.

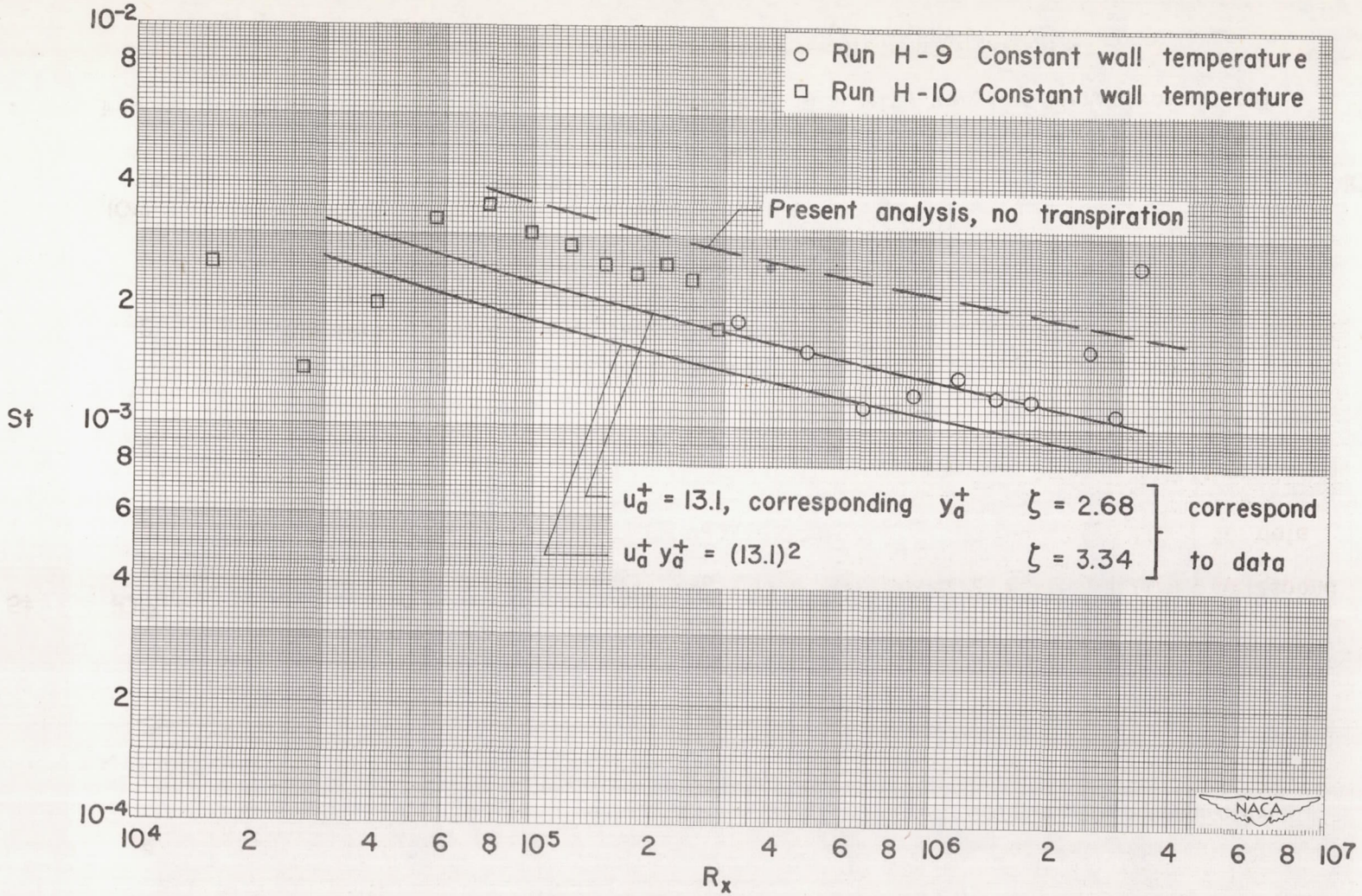

Figure 7.- Data of reference 9 for incompressible flow with varying transpiration rate $\frac{\rho_w v_w}{\rho_1 u_1} = \zeta\left(\frac{c_f}{2}\right)$ compared with present analysis.

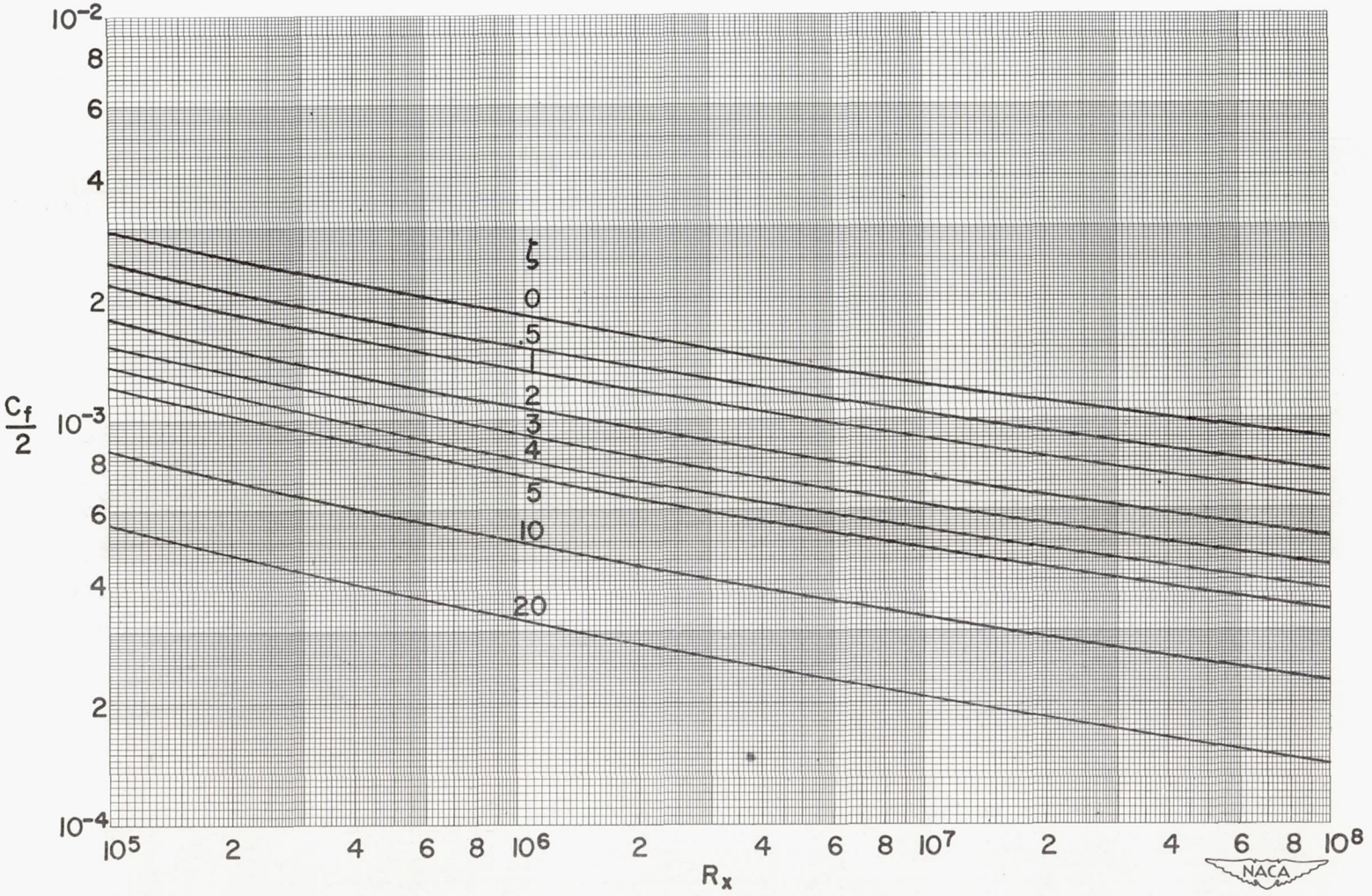

(a) M = 0; T_W = free-stream stagnation temperature.

Figure 8.- Effect of transpiration rate on local skin-friction coefficient.

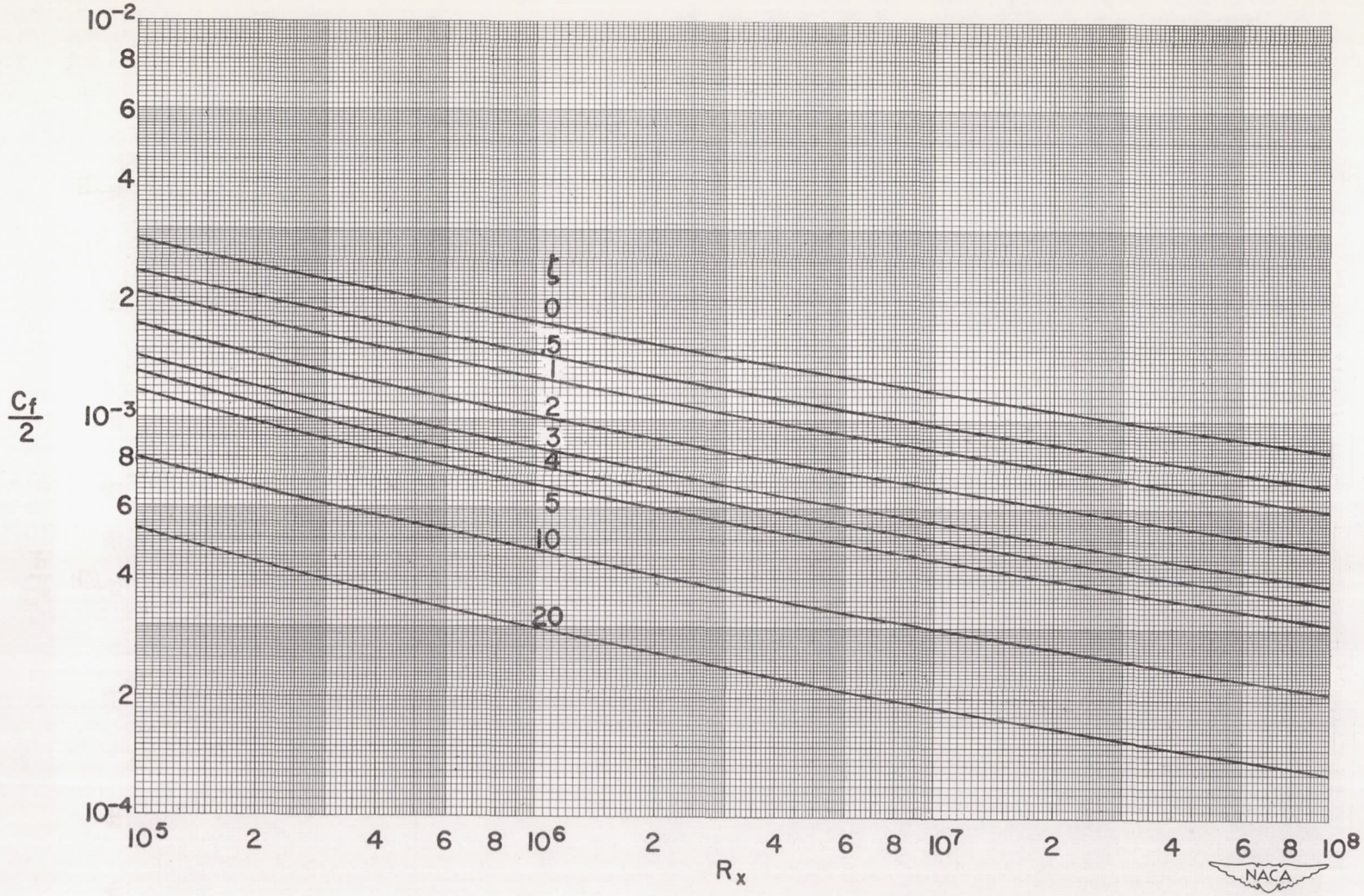

(b) M = 2; T_W = free-stream static temperature.

Figure 8.- Continued.

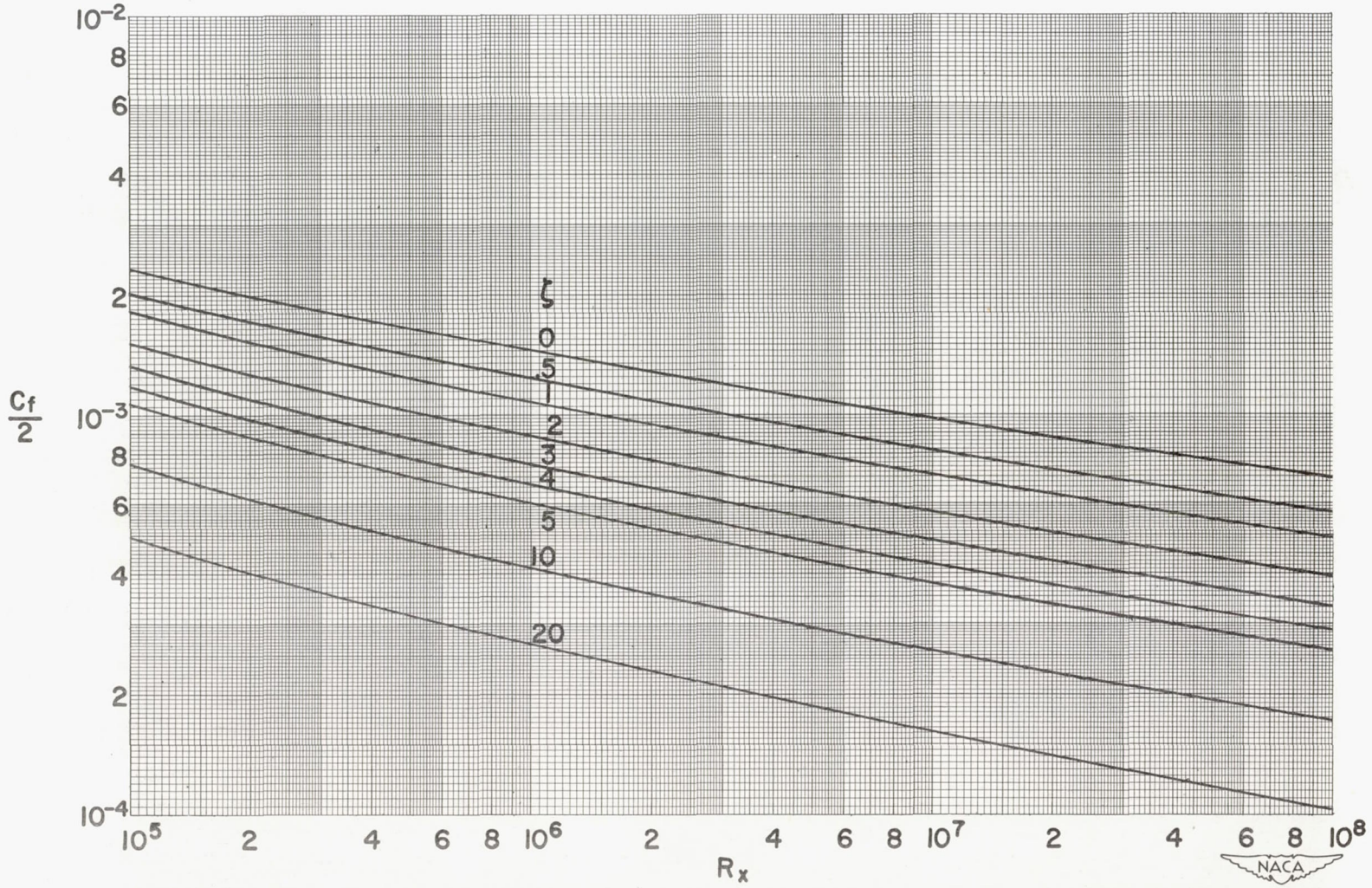

(c) M = 2; T_W = free-stream stagnation temperature.

Figure 8.- Continued.

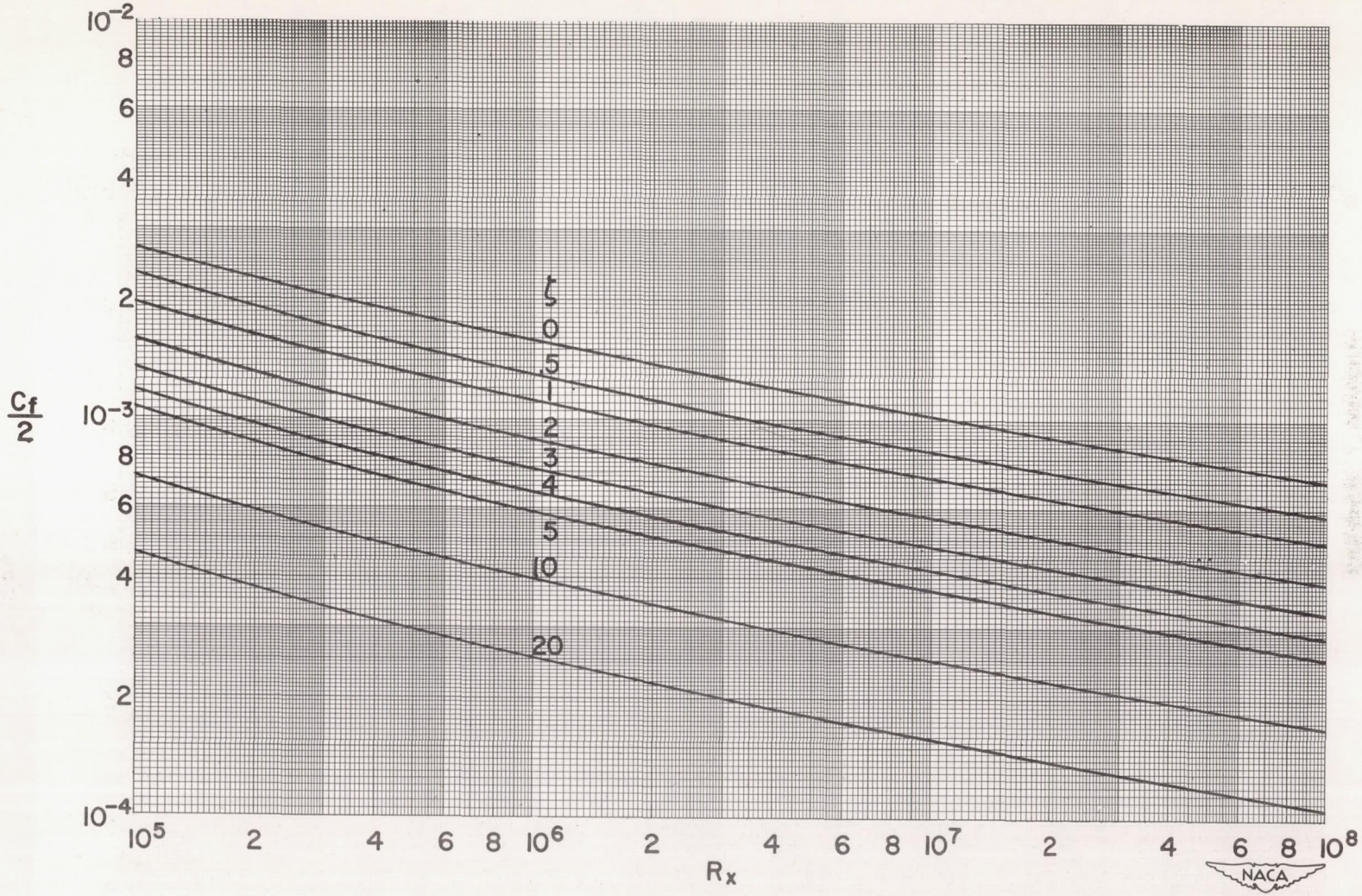

(d) M = 4; T_W = free-stream static temperature.

Figure 8.- Continued.

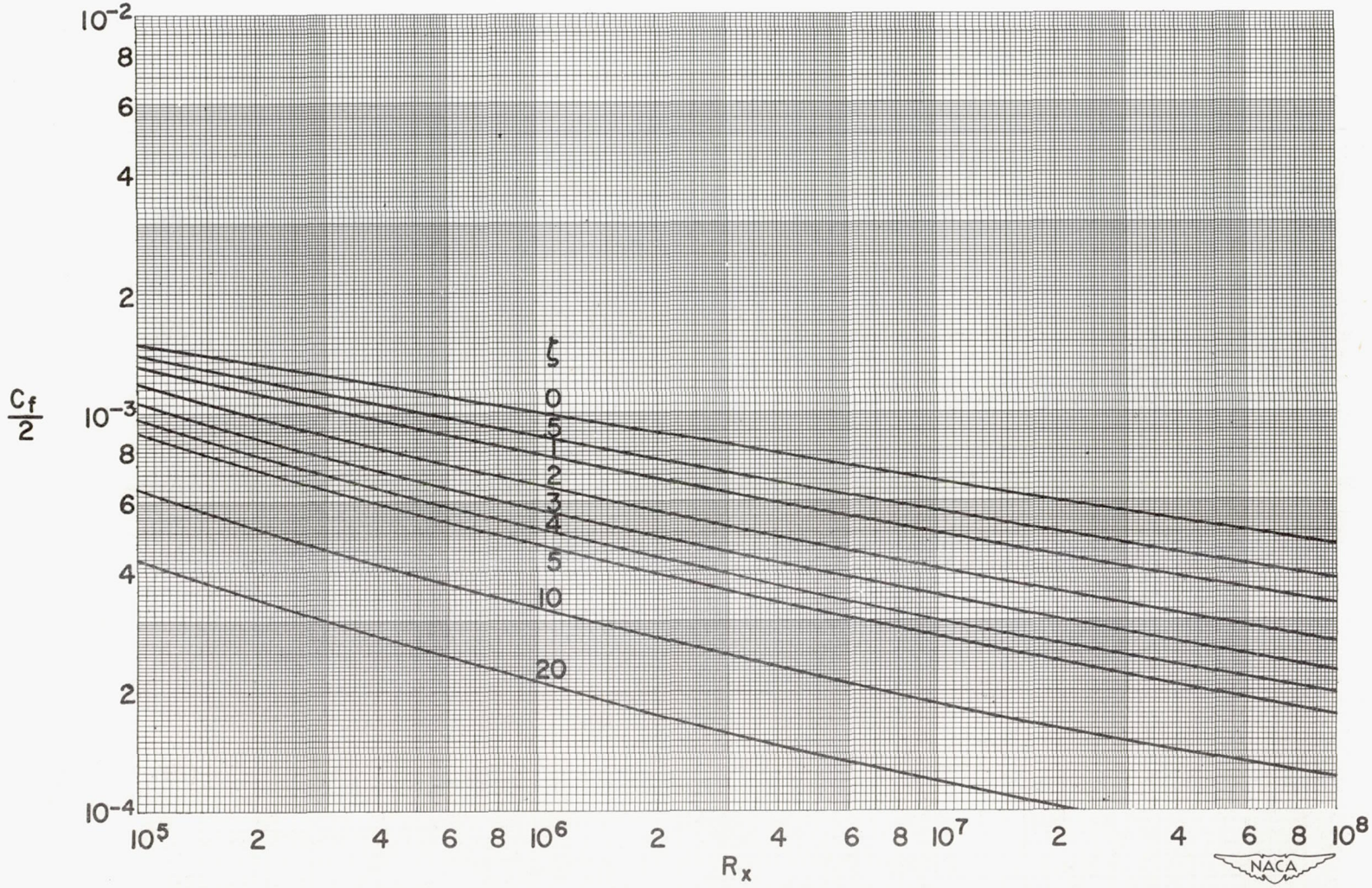

(e) M = 4; T_W = free-stream stagnation temperature.

Figure 8.- Concluded.

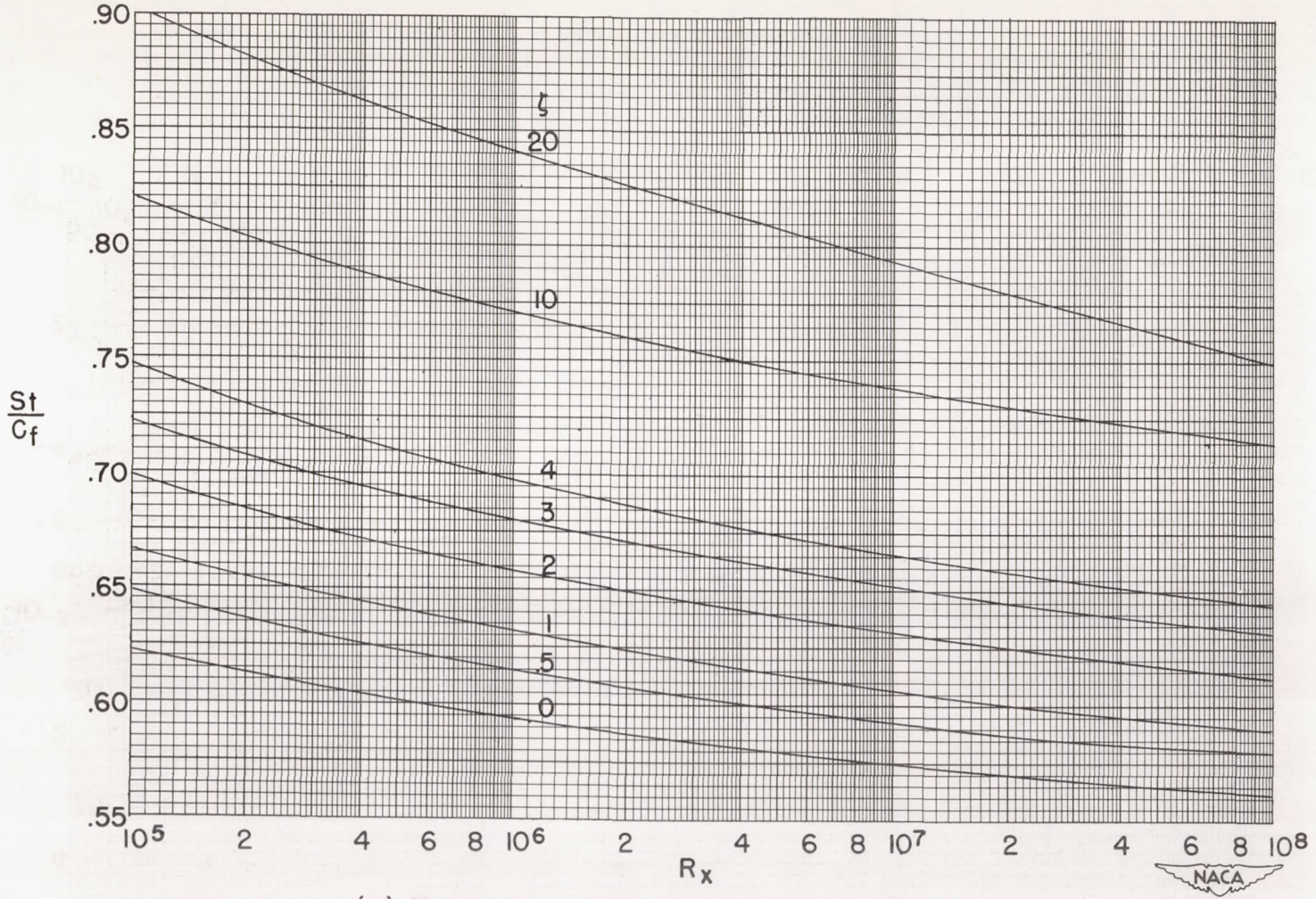

(a) M = 0; T_W = free-stream static temperature.

Figure 9.- Effect of transpiration rate on local ratio of Stanton number to skin-friction coefficient when $\frac{\rho_W v_W}{\rho_1 u_1} = \zeta\left(\frac{c_f}{2}\right)$.

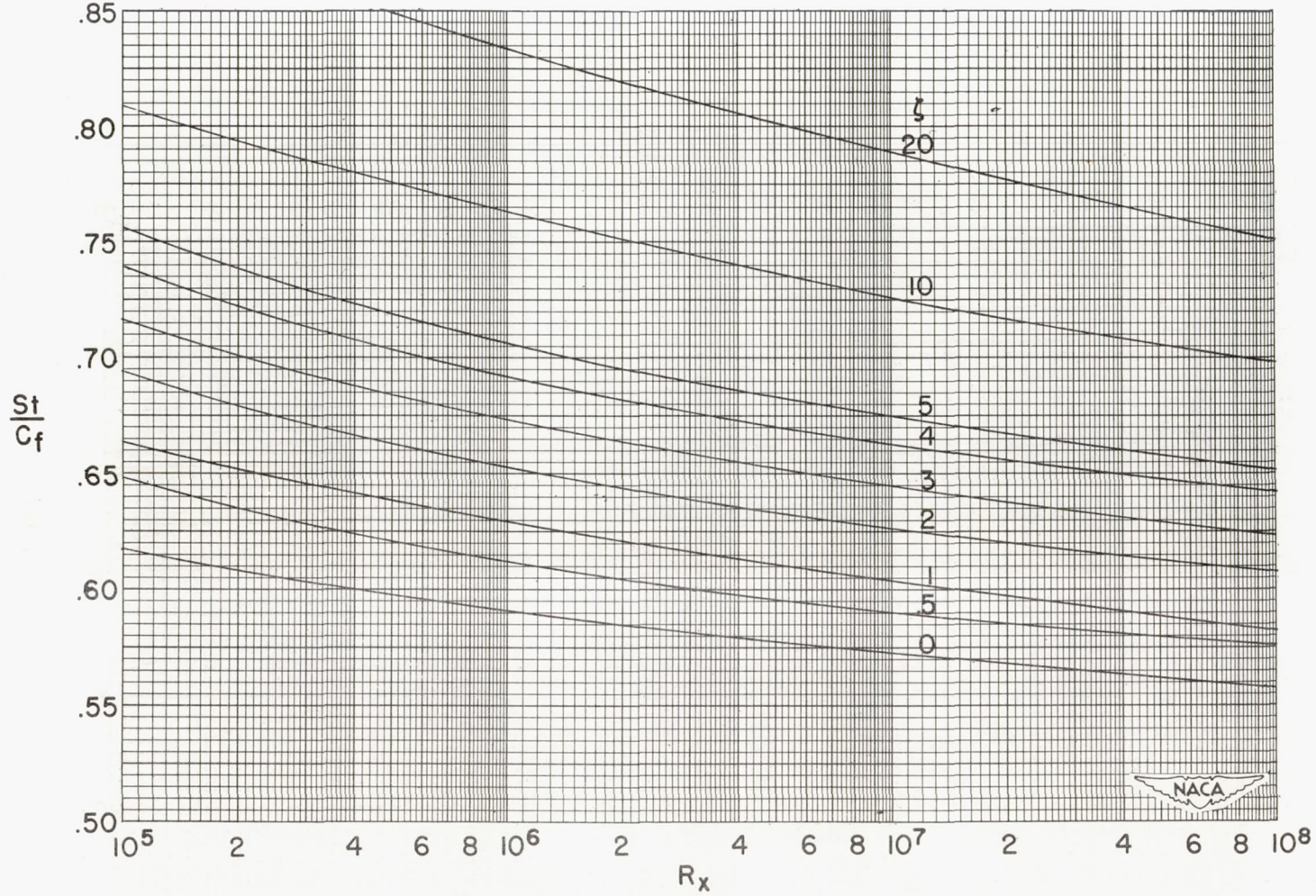

(b) M = 2; T_W = free-stream static temperature.

Figure 9.- Continued.

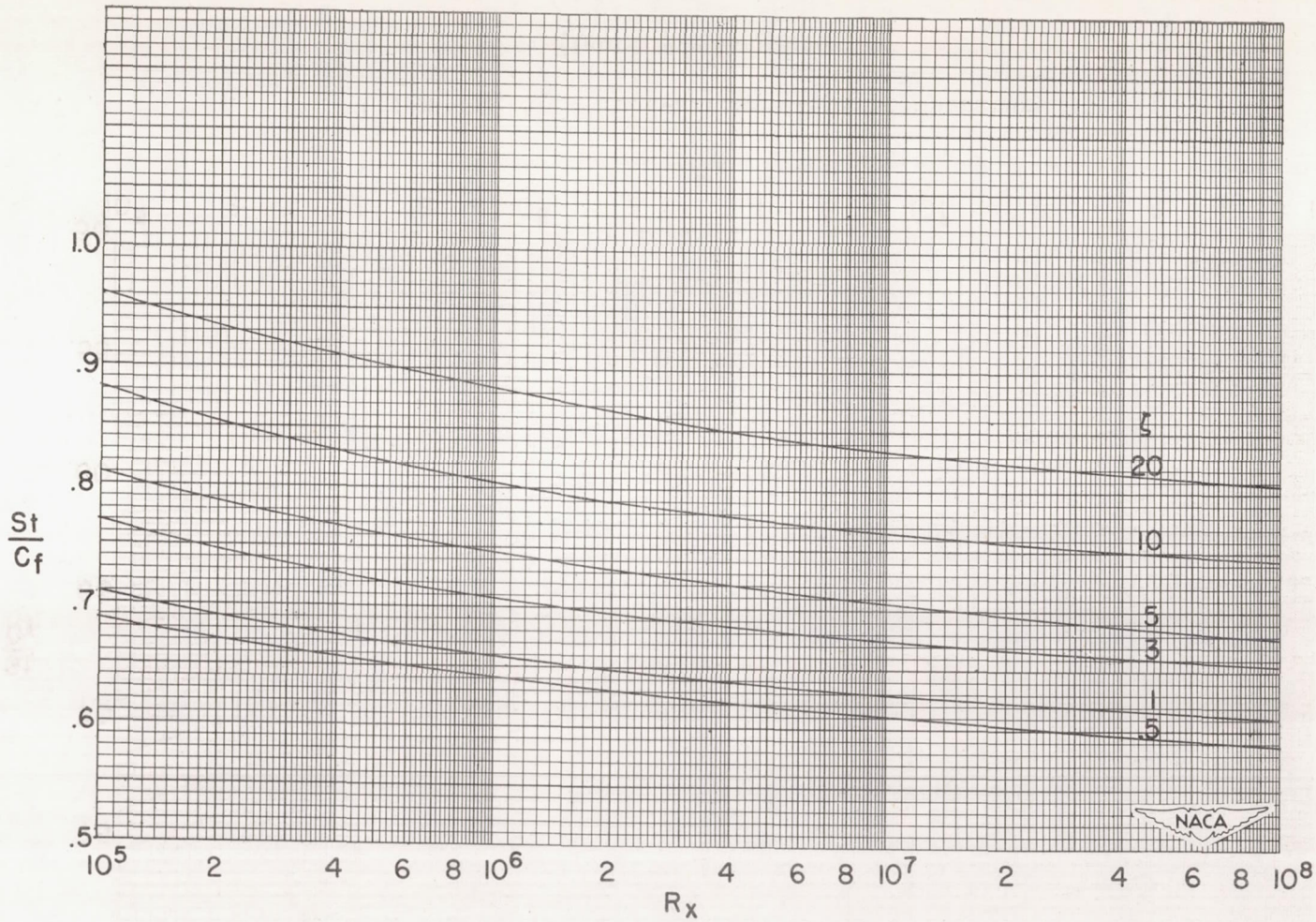

(c) M = 2; T_W = free-stream stagnation temperature.

Figure 9.- Continued.

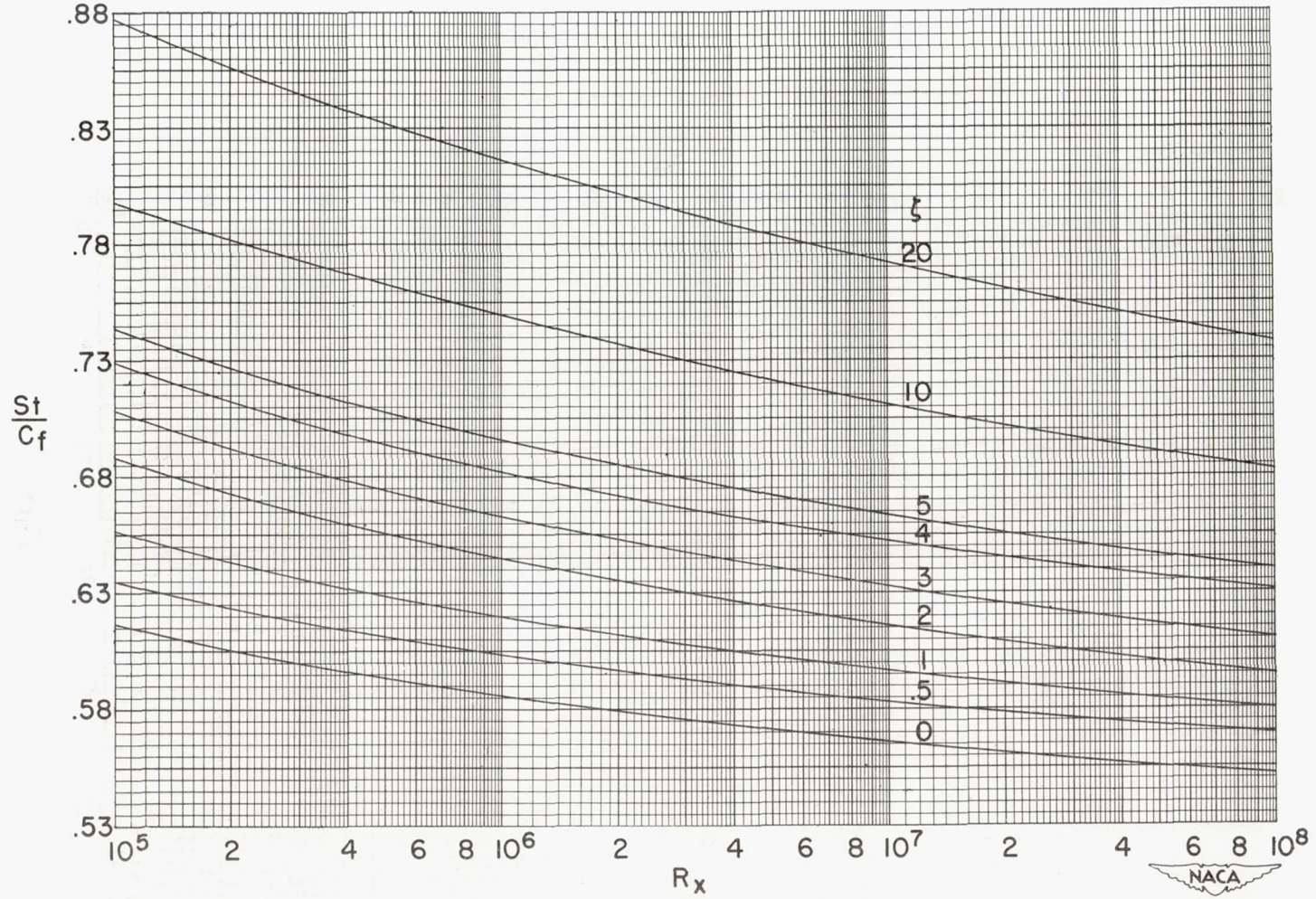

(d) M = 4; T_W = free-stream static temperature.

Figure 9.- Continued.

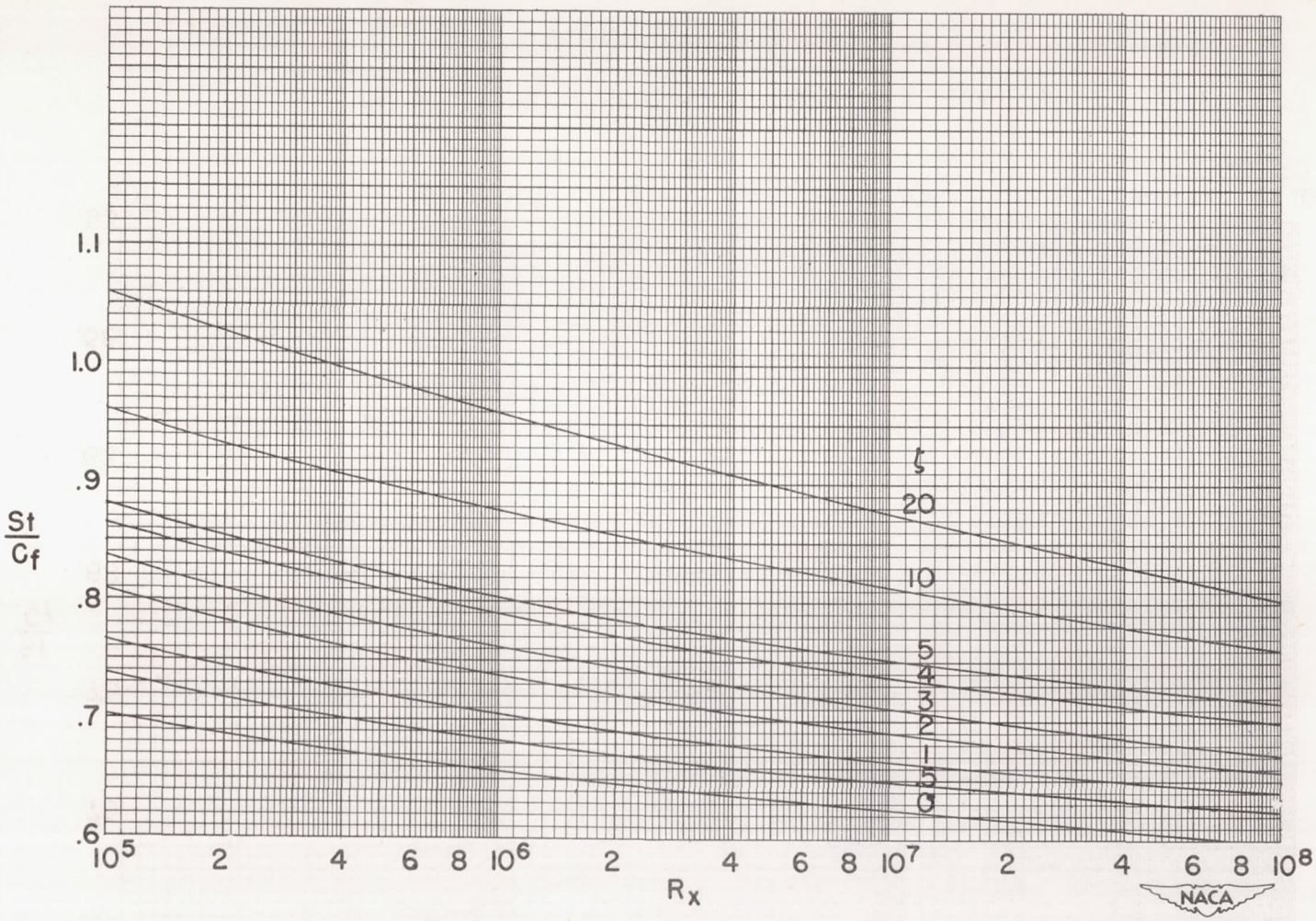

(e) M = 4; T_W = free-stream stagnation temperature.

Figure 9.- Concluded.

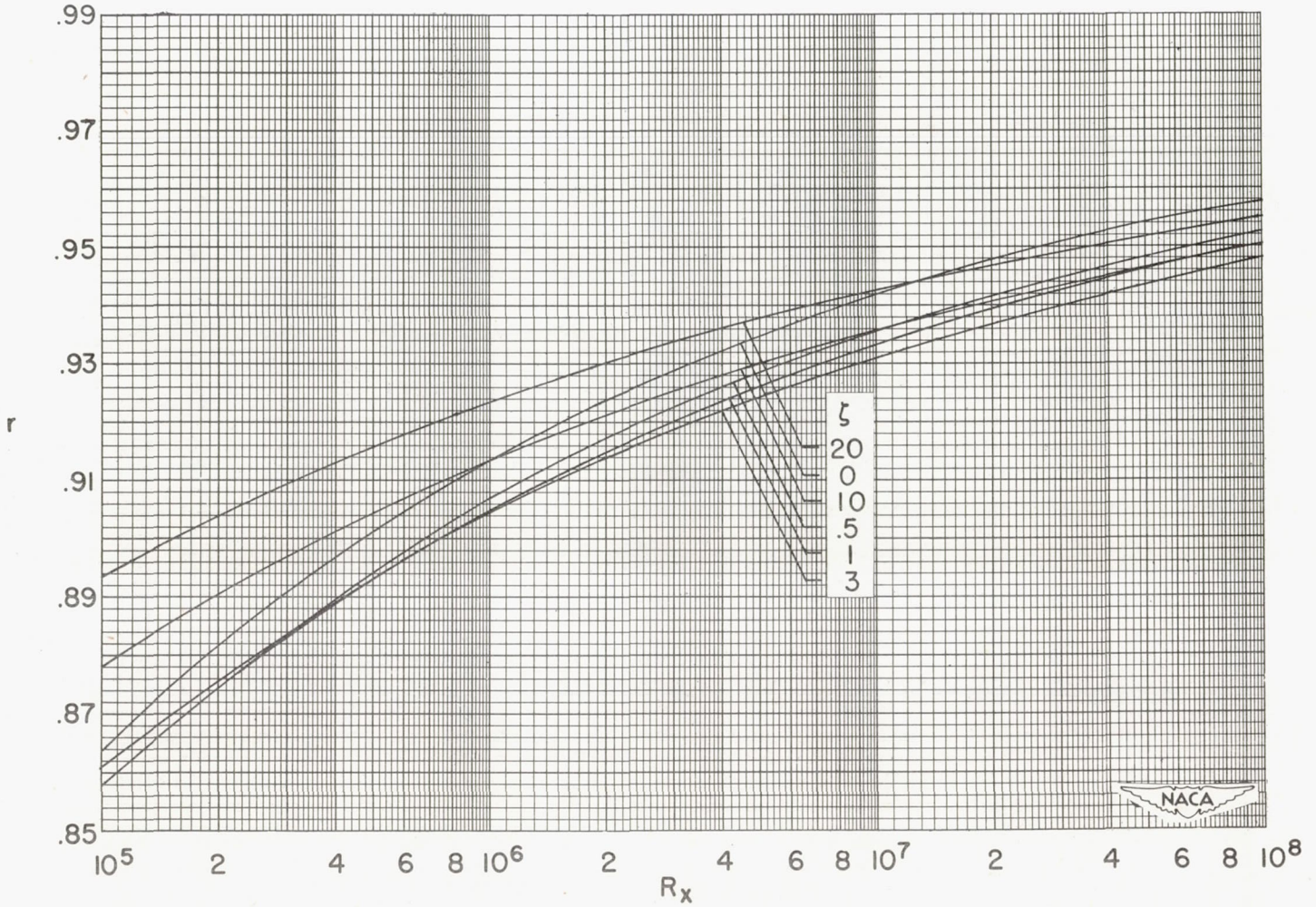

Figure 10.- Effect of transpiration rate on local temperature recovery factor at Mach number of 0 when $\frac{\rho_w v_w}{\rho_1 u_1} = \zeta\left(\frac{c_f}{2}\right)$.

NACA-Langley - 12-1-54 - 1000